

# Accepted Manuscript

Rational approach to highly potent and selective apoptosis signal-regulating kinase 1 (ASK1) inhibitors

Frank Lovering, Paul Morgan, Christophe Allais, Ann Aulabaugh, Joanne Brodfuehrer, Jeanne Chang, Jotham Coe, WeiDong Ding, Heather Dowty, Margaret Fleming, Richard Frisbie, Julia Guzova, David Hepworth, Jayasankar Jasti, Steve Kortum, Ravi Kurumbail, Shashi Mohan, Nikolaos Papaioannou, Joseph W. Strohbach, Fabien Vincent, Katherine Lee, Christoph W. Zapf



PII: S0223-5234(17)31068-1

DOI: [10.1016/j.ejmech.2017.12.041](https://doi.org/10.1016/j.ejmech.2017.12.041)

Reference: EJMECH 10019

To appear in: *European Journal of Medicinal Chemistry*

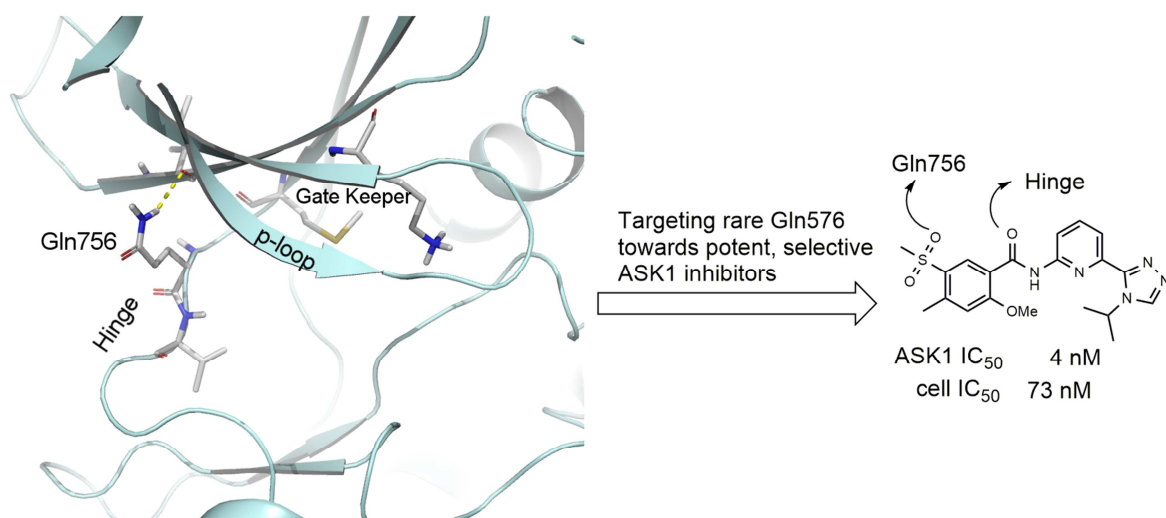
Received Date: 27 October 2017

Revised Date: 11 December 2017

Accepted Date: 13 December 2017

Please cite this article as: F. Lovering, P. Morgan, C. Allais, A. Aulabaugh, J. Brodfuehrer, J. Chang, J. Coe, W. Ding, H. Dowty, M. Fleming, R. Frisbie, J. Guzova, D. Hepworth, J. Jasti, S. Kortum, R. Kurumbail, S. Mohan, N. Papaioannou, J.W. Strohbach, F. Vincent, K. Lee, C.W. Zapf, Rational approach to highly potent and selective apoptosis signal-regulating kinase 1 (ASK1) inhibitors, *European Journal of Medicinal Chemistry* (2018), doi: 10.1016/j.ejmech.2017.12.041.

This is a PDF file of an unedited manuscript that has been accepted for publication. As a service to our customers we are providing this early version of the manuscript. The manuscript will undergo copyediting, typesetting, and review of the resulting proof before it is published in its final form. Please note that during the production process errors may be discovered which could affect the content, and all legal disclaimers that apply to the journal pertain.



ACCEPTED MANUSCRIPT

## Rational Approach to Highly Potent and Selective Apoptosis Signal-Regulating Kinase 1 (ASK1) inhibitors

.....

Frank Lovering<sup>1</sup>, Paul Morgan<sup>2</sup>, Christophe Allais<sup>1</sup>, Ann Aulabaugh<sup>1</sup>, Joanne Brodfuehrer<sup>3</sup>, Jeanne Chang<sup>1</sup>, Jotham Coe<sup>1</sup>, WeiDong Ding<sup>1</sup>, Heather Dowty<sup>4</sup>, Margaret Fleming<sup>2</sup>, Richard Frisbie<sup>1</sup>, Julia Guzova<sup>2</sup>, David Hepworth<sup>1</sup>, Jayasankar Jasti<sup>1</sup>, Steve Kortum<sup>1</sup>, Ravi Kurumbail<sup>1</sup>, Shashi Mohan<sup>2</sup>, Nikolaos Papaioannou<sup>1</sup>, Joseph W. Strohbach<sup>1</sup>, Fabien Vincent<sup>1</sup>, Katherine Lee<sup>1</sup>, Christoph W. Zapf<sup>1</sup>

<sup>1</sup>Medicine Design, <sup>2</sup>Inflammation and Immunology, <sup>3</sup>Biomedicine Design, <sup>4</sup>Drug Safety Research and Development

\*\*\*\*\*

Pfizer, Inc.  
1 Portland Street, Cambridge, MA 02139, USA  
445 Eastern Point Road, Groton, CT 06340, USA

E-mail: frank.lovering@pfizer.com

\*\*\*\*\*

## Abstract

Many diseases are believed to be driven by pathological levels of reactive oxygen species (ROS) and oxidative stress has long been recognized as a driver for inflammatory disorders. Apoptosis signal-regulating kinase 1 (ASK1) has been reported to be activated by intracellular ROS and its inhibition leads to a down regulation of p38- and JNK-dependent signaling. Consequently, ASK1 inhibitors may have the potential to treat clinically important inflammatory pathologies including renal, pulmonary and liver diseases. Analysis of the ASK1 ATP-binding site suggested that Gln756, an amino acid that rarely occurs at the GK+2 position, offered opportunities for achieving kinase selectivity for ASK1 which was applied to the design of a parallel medicinal chemistry library that afforded inhibitors of ASK1 with nanomolar potency and excellent kinome selectivity. A focused optimization strategy utilizing structure-based design resulted in the identification of ASK1 inhibitors with low nanomolar potency in a cellular assay, high selectivity when tested against kinase and broad pharmacology screening panels, and attractive physicochemical properties. The compounds we describe are attractive tool compounds to inform the therapeutic potential of ASK1 inhibition.

## Introduction

The mitogen-activated protein kinase (MAPK) pathway is an important intracellular signaling system that regulates diverse cellular functions, such as proliferation, differentiation, and apoptosis.<sup>1</sup> Apoptosis signal-regulating kinase 1 (ASK1), also known as mitogen-activated protein kinase kinase kinase 5 (MAP3K5), is an ubiquitously expressed member of MAPK kinase kinases regulating Jun N-terminal kinase (JNK) and p38 signaling.<sup>2-4</sup> ASK1 is preferentially activated in response to various stimuli including reactive oxygen species (ROS), lipopolysaccharide (LPS), tumor necrosis factor- $\alpha$  (TNF- $\alpha$ ), mitochondrial dysfunction and endoplasmic reticulum (ER) stress.<sup>5-8</sup> The redox regulation of ASK1 occurs via thioredoxin (TRX) which is covalently bound to the N-terminal region of ASK1 through a disulfide bond.<sup>9</sup>

Under conditions such as oxidative stress, ROS induced liberation of TRX from ASK1 leads to ASK1 homodimerization<sup>10</sup> and the phosphorylation of the critical threonine residue (Thr838) in the activation loop of ASK1.<sup>11</sup>

A number of studies using ASK1-deficient mice suggest that ASK1 has important functions in oxidative stress-related diseases. ASK1<sup>-/-</sup> mice display a protective phenotype in multiple disease models including asthma<sup>12</sup>, acute kidney injury<sup>13</sup>, neurodegenerative disorders<sup>8</sup>, cardiovascular<sup>14, 15</sup>, inflammatory<sup>16</sup>, and metabolic disorders<sup>17</sup>. Thus, it is thought that small molecule compounds inhibiting ASK1 could be used for the treatment of these pathologies. Recent studies suggest that ASK1 inhibitors may be protective in rodent models of ischemia-reperfusion injury,<sup>18</sup> dilated cardiomyopathy,<sup>19</sup> diabetic nephropathy,<sup>20</sup> and hepatotoxic liver injury.<sup>21</sup>

Several ASK1 inhibitors have been disclosed in the public domain (Figure 1). Imidazopyridine **1** was recently reported to inhibit ASK1 with an IC<sub>50</sub> of 14 nM.<sup>22</sup> Subsequently, additional ASK1 inhibitors have been described in the patent literature with compounds **2**<sup>23</sup> and **3**<sup>24</sup> as representative examples from their respective filings, while analog **4** was the sole compound reported in a patent application<sup>25</sup> and was recently reported to be in clinical trials as GS-4997/selonsertib for diabetic kidney disease and nonalcoholic steatohepatitis (NASH).<sup>26</sup>

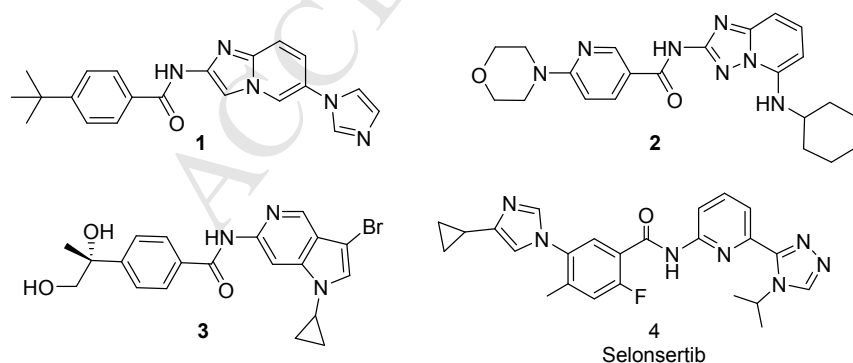


**Figure 1:** Representative ASK1 inhibitors **1-4** from the literature.

### Structural Analysis

We sought tool compounds with selective inhibition of ASK1 to help build our understanding of the pharmacology of ASK1. An analysis of the ATP binding site of ASK1 was conducted to identify unique structural features in order to enhance the kinome selectivity of new compounds. Targeting distinctive kinase features such as binding pockets or side chains in the design of kinase inhibitors is a strategy to increase kinome selectivity.

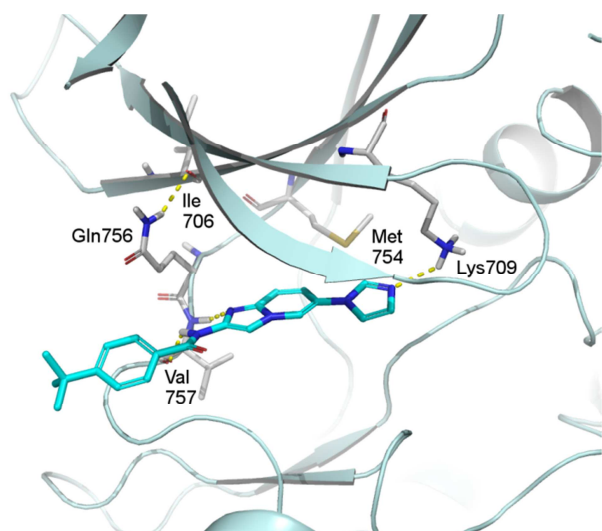


**Figure 2:** Protein crystal structure of literature compound **1** (PDB 3VW6)<sup>22</sup> reveals an unusual Gln756 at the GK+2 position of the hinge which engages in an intra-protein hydrogen bond with the backbone carbonyl of Ile706.

An analysis of the ATP-binding site revealed that most of the amino acids in each position of the ASK1 active site frequently occur in other kinases as well. For example, 182 of the 442 kinases examined, including ASK1, share a methionine as the “gatekeeper” residue (Figure 2). In contrast, Gln756 (at the GK+2 position using the nomenclature of Ghose et al<sup>27</sup>) has a very low abundance in this particular position of the ATP binding site of kinases. Only 3 kinases feature a Gln at the GK+2 position: ASK1 (MEKK5, MAP3K5), TAK1 (MAP3K7), and PIK3R4. Inspection of a crystal structure<sup>22</sup> of imidazopyridine **1** bound in the active site of ASK1 revealed that the side-chain of Gln756 engages the backbone carbonyl

of Ile706 in an intra-protein hydrogen bond. It was speculated that this interaction widens the channel at the hinge, allowing the t-Bu phenyl moiety of compound **1** to move past the Gln756 side chain and access space commonly inaccessible.

This distinguishing feature of the ASK1 pocket within the kinome was effectively demonstrated from the overlay of crystal structures of ~4800 kinase inhibitors from the Pfizer database into the ATP active site of ASK1 (Figure 3; For clarity Figure 3 was prepared by clustering the 4800 inhibitors to 1000 clusters and the cluster centers were kept). It was noted that inhibitor **1** emerges from this ensemble of kinase inhibitors to occupy this unusual selectivity channel adjacent to Gln756. This observation, in addition to the fact that the GK+2 position is rarely populated by the polar amino acid glutamine led to the design hypothesis that (1) accessing this unique channel, as observed for compound **1**, with small molecules while simultaneously (2) interacting with Gln756 at the GK+2 position would lead to potent and highly selective ASK1 inhibitors.

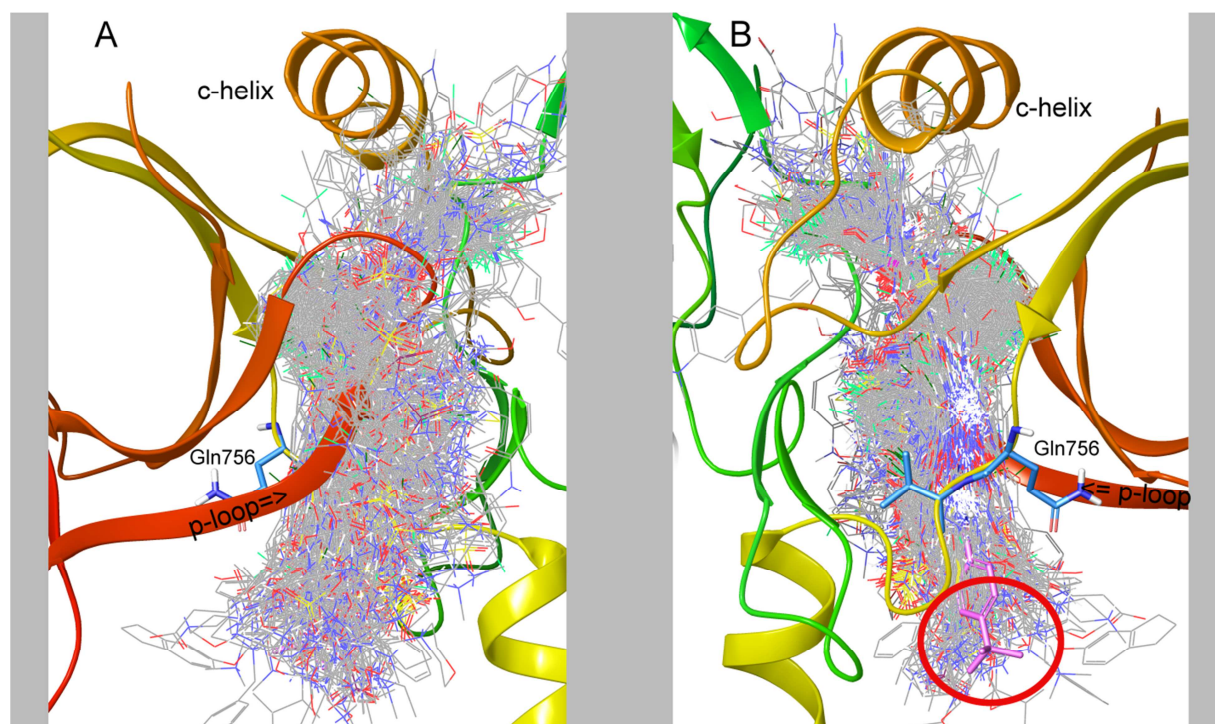


**Figure 3:** Protein crystal structure of literature compound **1** (PDB 3VW6)<sup>22</sup> overlaid with approximately 1000 kinase inhibitor co-crystal structures from the Pfizer database. (A) illustrates the traditional view of the kinase site with the p-loop labeled. (B) is rotated 180° to illustrate that imidazopyridine **1** occupies rather unique space across the kinome (red circle).

Analysis of ASK1 crystal structures as well as an investigation of how compound **4** might bind were undertaken to understand opportunities for engaging Gln756. To this end a docking model derived from PDB 3VW6<sup>22</sup> was used to predict the binding mode of amide **4** in the ASK1 active site as shown in Figure 4. Instead of interacting with the hinge through the hydrogen bond donor and acceptor motif of the amino-pyridine moiety, amide **4** was predicted to act as a single-point hinge binder with its amide carbonyl engaging the NH of Val757. In light of a recent analysis on kinome selectivity, a single-point hinge binding motif may be preferable to a two-point hinge binder to increase the probability of achieving kinome selectivity.<sup>28</sup>

In addition to the hinge contact, the docking model suggested a productive interaction of the triazole with Lys709 and a non-classical hydrogen-bond interaction between the imidazole C<sub>5</sub>-H and the carbonyl of Gln756 (3.3 Å). Having identified amide **4** as an inhibitor which features key criteria for its target engagement such as being a single-point hinge binder and displaying an interaction with Gln756, efforts were directed toward expanding the chemical space around this compound. Specifically we sought to maintain the single point hinge binding characteristics while exploring which other moieties might engage Gln756.

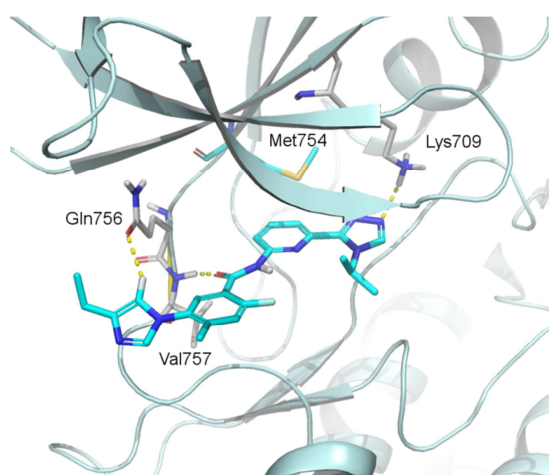


**Figure 4:** Docking pose of compound **4** in ASK1. Amide **4** is predicted by the docking model to interact with the amide carbonyl of Val757 of the hinge through its amide carbonyl, the conserved Lys709 through the triazole N3, as well as a non-classical hydrogen bond between the carbonyl of Gln756 and the imidazole C<sub>5</sub>-H.

#### Library design

A virtual amide library was enumerated by acylating the *iPr*-triazole-substituted 2-amino-pyridine moiety with available carboxylic acids (Figure 6). The goal of this library was to identify ASK1 inhibitors which would engage either rotamer of the carboxamide side-chain of Gln756, thus targeting either the

NH<sub>2</sub> or the C=O group with a range of functional groups. In addition, substituents were sought that provided a vector to access the selectivity channel occupied by the tert-butyl phenyl moiety in amide **1**.

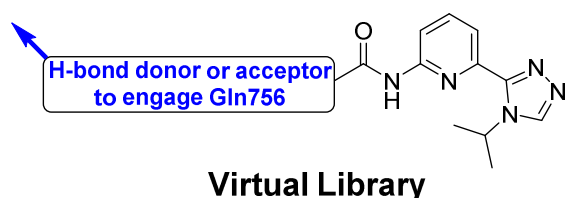


**Figure 5:** Library design to identify ASK1 inhibitors targeting Gln756.

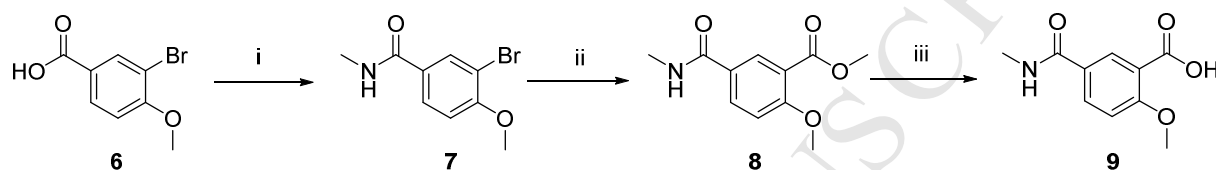
To this end, a virtual library of more than 14,000 amide analogs was enumerated and docked into the ATP-binding site of ASK1 using a docking model derived from **1** (pdb code 3VW6) wherein each of the two Gln756 rotamers were sampled. This effort led to the prioritization of 29 chemically diverse analogs for synthesis which were expected to deliver highly potent and selective ASK1 inhibitors.

### Synthesis of Potential Inhibitors

The compounds in Tables 1-3 were prepared by amide bond coupling of the appropriately substituted benzoic acid fragments with 6-(4-isopropyl-4H-1,2,4-triazol-3-yl)pyridin-2-amine (**5**). Preparation of the substituted benzoic acid fragments not commercially available is outlined in Schemes 1 and 2. 2-Methoxy-5-(methylcarbamoyl)benzoic acid (**9**) was prepared by the amide coupling of 3-bromo-4-methoxybenzoic acid (**6**) with methylamine to afford **7**. Palladium catalyzed carbonylation of **7** under 50 psi CO in methanol / DMF (1:1) provided ester **8**. The ester hydrolysis was accomplished using lithium hydroxide in aqueous methanol to give compound **9** (Scheme 1). 2-Methoxy-4-methyl-5-sulfamoylbenzoic acid (**12**) was prepared by treatment of **10** with thionyl chloride and chlorosulfonic acid to afford **11**. The sulfonyl chloride was dissolved in ammonium hydroxide and acidified to give **12** (Scheme 2). **16** was prepared by treating **11** with acetic acid at 90°C followed by reduction with tin

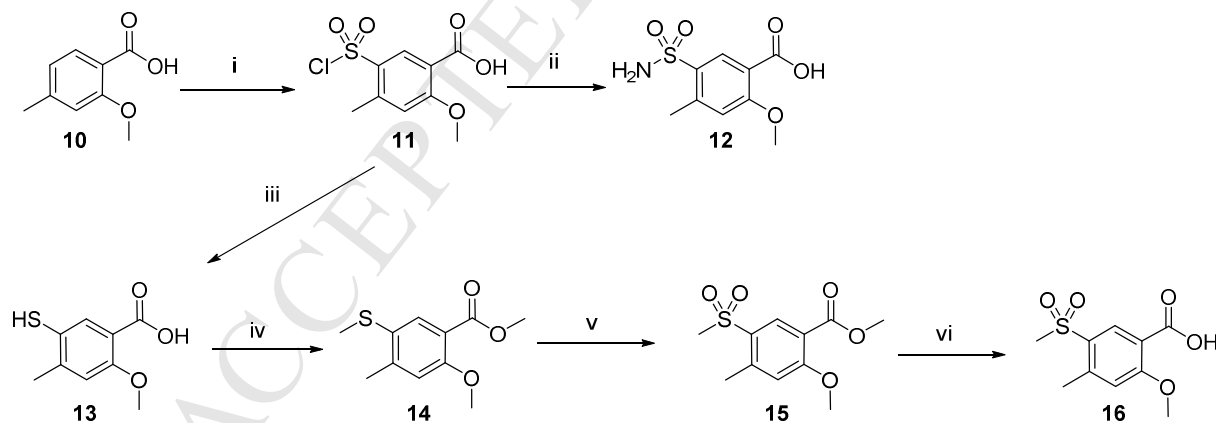
metal in hydrochloric acid at 45°C to give the thiol **13**. The thiol was alkylated with iodomethane in acetone with potassium carbonate as base to afford the thioether **14**. The thioether was oxidized with potassium permanganate in a biphasic reaction to give **15** followed by ester hydrolysis to provide **16** (Scheme 2).

### Scheme 1. Synthesis of Intermediate 9<sup>a</sup>



<sup>a</sup>Reagents and conditions: (i) EDCI, HOBT, diisopropylethylamine, methylamine hydrochloride, DCM, rt, 18 h, 100%. (ii) trimethylamine, palladium acetate, 1,3-bis(diphenylphosphino)propane, DMF, MeOH, CO 50psi, 80°C, 16 h, 91%. (iii) lithium hydroxide, MeOH, water, rt, 1 h, 78%.

### Scheme 2. Synthesis of Intermediates 12 and 16<sup>a</sup>

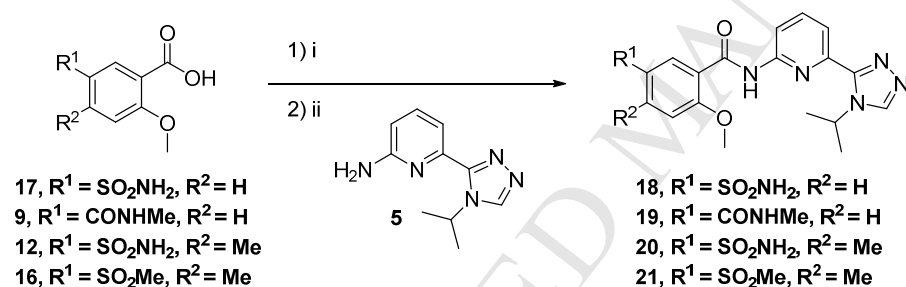


<sup>a</sup>Reagents and conditions: (i) ClSO<sub>3</sub>H, DCM, thionyl chloride, -5 to -20°C, 5 h, 61%. (ii) NH<sub>4</sub>OH, 0°C, 5 min., 43%. (iii) AcOH, 90°C, 10 min, Sn, HCl, 45°C-60°C, 2 h, 99%. (iv) MeI, K<sub>2</sub>CO<sub>3</sub>, acetone, 50°C, 16 h, 26%. (v)

benzoic acid, benzyltriethylammonium chloride, DCM,  $\text{KMnO}_4$ , water,  $20^\circ\text{C}$ , 3 h, 75%. (vi) LiOH monohydrate, THF, water, EtOH,  $20^\circ\text{C}$ , 5 h, HCl, 100%.

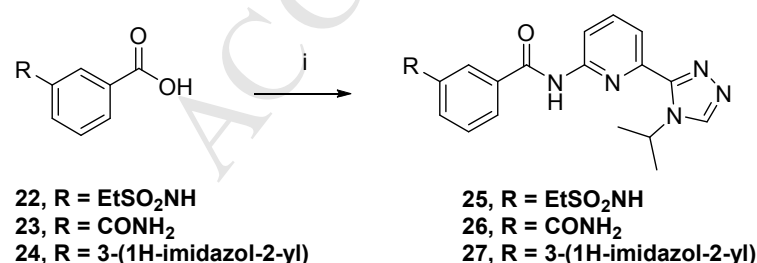
Compounds **18-21** were synthesized by conversion of the appropriate acid to the acid chloride using oxalyl chloride and subsequent addition of **5** in pyridine (Scheme 3). Compounds **25-27** were synthesized in a library format by coupling the commercially available acids with 6-(4-isopropyl-4H-1,2,4-triazol-3-yl)pyridin-2-amine using propylphosphonic anhydride (T3P) with triethylamine at  $100^\circ\text{C}$  (Scheme 4).

### Scheme 3. Synthesis of Compounds 18-21<sup>a</sup>



<sup>a</sup>Reagents and conditions: (i) MeCN, oxalyl chloride, DMF, rt, 1 h. (ii) 6-(4-isopropyl-4H-1,2,4-triazol-3-yl)pyridin-2-amine (**5**), pyridine, rt, 18 h, 6-99%.

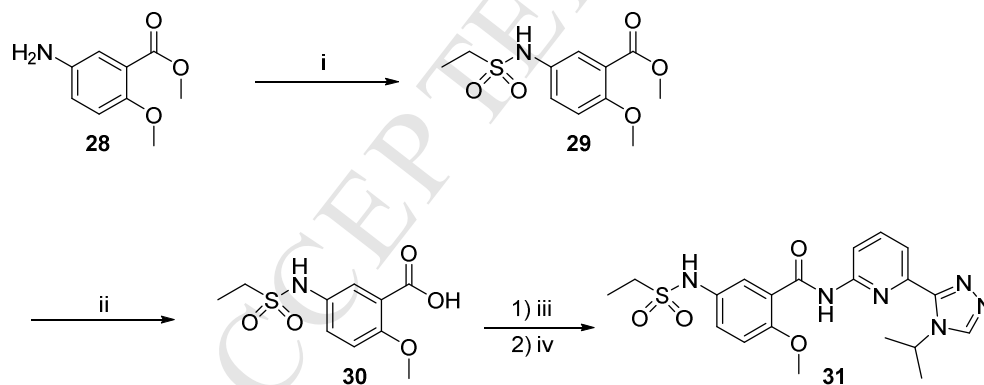
### Scheme 4. Synthesis of Compounds 25-27<sup>a</sup>



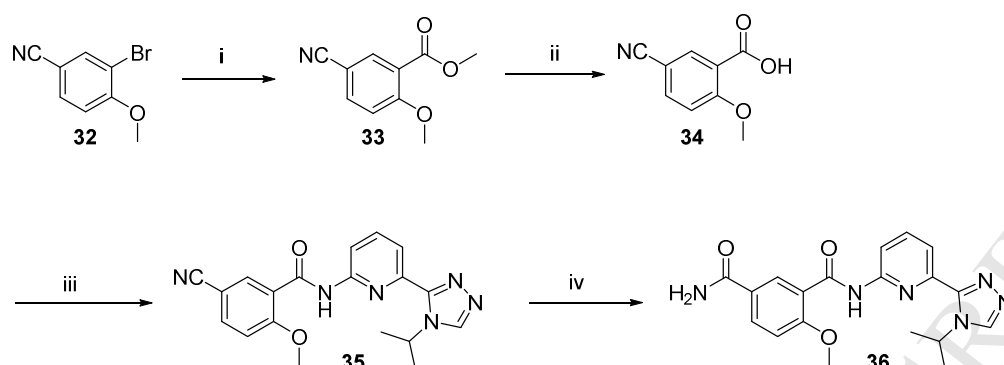
<sup>a</sup>Reagents and conditions: (i) T3P (50% in EtOAc), triethylamine, **5**,  $100^\circ\text{C}$ , 16 h.

Compound **31** was synthesized by reacting 5-amino-2-methoxybenzoate (**28**) with ethanesulfonyl chloride in the presence of pyridine in DCM to give sulfonamide **29**. Hydrolysis of **29** by aqueous sodium hydroxide afforded the acid **30** which was converted to the acid chloride by heating in thionyl chloride. Residual thionyl chloride was removed under reduced pressure and the crude acid chloride reacted with **5** in acetonitrile at room temperature. The resulting precipitate was recrystallized from methanol to provide compound **31** (Scheme 5). Compound **36** was synthesized by the palladium catalyzed carbonylation of 3-bromo-4-methoxybenzonitrile (**32**) in methanol under 60 psi CO to give ester **33**. Hydrolysis with lithium hydroxide and amide coupling with **5** using Mukaiyama's reagent<sup>29</sup> afforded the nitrile **35** which was treated with hydrogen peroxide and potassium carbonate to provide **36** (Scheme 6). Compound **38** was synthesized by converting the commercially available acid 2-methoxy-5-(methylsulfonyl)benzoic acid (**37**) to the acid chloride with thionyl chloride and reacting with **5** in pyridine at room temperature (Scheme 7).

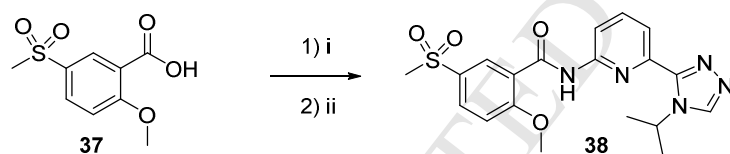
#### Scheme 5. Synthesis of Compound **31**<sup>a</sup>



<sup>a</sup>Reagents and conditions: (i) pyridine, ethanesulfonyl chloride, rt, 2 h, 96%. (ii) NaOH, THF, water, rt, 4 h, 78%. (iii) thionyl chloride, 50°C, 1 h. (iv) **5**, rt, 16 h, MeOH, 33%.

Scheme 6, Synthesis of Compound 36<sup>a</sup>

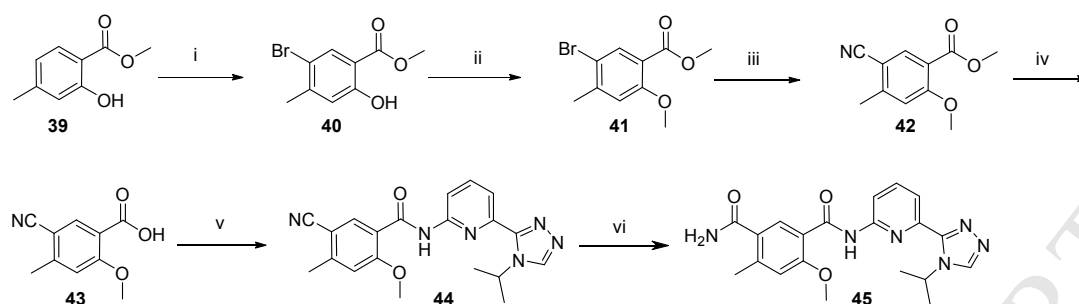
<sup>a</sup>Reagents and conditions: (i) triethylamine, Pd(dppf)Cl<sub>2</sub>, MeOH, CO (60 psi), 100°C, 4 h, 22%. (ii) lithium hydroxide monohydrate, THF, water, rt, 4 h, 81%. (iii) **5**, diisopropylethylamine, Mukaiyama's reagent, THF, 70°C, 4 h, 97%. (iv) DMSO, K<sub>2</sub>CO<sub>3</sub>, H<sub>2</sub>O<sub>2</sub>, rt, 30 min., 10%.

Scheme 7, Synthesis of Compound 38<sup>a</sup>

<sup>a</sup>Reagents and conditions: (i) thionyl chloride, 1 h, 55°C. (ii) **5**, pyridine, rt, 2 h, NaOH, 60°C, 6N HCl, rt, 1 h, 35%.

Compound **45** was synthesized by bromination of methyl-2-hydroxy-4-methyl benzoate (**39**) followed by phenol alkylation with methyl iodide to give **41**. Palladium catalyzed cyanation with zinc cyanide was used to obtain **42**. Ester hydrolysis using sodium hydroxide followed by amide coupling and treatment of the nitrile with hydrogen peroxide and potassium carbonate afforded the primary amide **45** (Scheme 8).

Scheme 8, Synthesis of compound 45<sup>a</sup>



<sup>a</sup>Reagents and conditions: (i) Br<sub>2</sub>, CHCl<sub>3</sub>, 0°C, 3 h, 95%. (ii) MeCN, MeI, K<sub>2</sub>CO<sub>3</sub>, 40°C, 16 h, 17%. (iii) Zn(CN)<sub>2</sub>, Xantphos, Pd<sub>2</sub>(dba)<sub>3</sub>, N,N,N',N'-tetramethylethylenediamine, DMF, 160°C, 200 s, 92%. (iv) MeOH, water, NaOH, rt, 30 h, HCl, 95%. (v) MeCN, DMF, oxalyl chloride, 1 h, rt, 5, pyridine, rt, 2 h, 85%. (vi) H<sub>2</sub>O<sub>2</sub>, K<sub>2</sub>CO<sub>3</sub>, DMSO, rt, 30 min., 5%.

### In-Vitro Assays

Inhibitor efficacy was evaluated using a homogeneous time-resolved fluorescence (HTRF) assay that measures the phosphorylation of a peptide substrate by recombinant human full-length ASK1. In order to best reflect the physiological intracellular environment, a 1 mM concentration of ATP in the assay was employed. As some compounds were potent and approached the limits of the assay as defined by the concentration of enzyme (3 nM), the  $K_i^{\text{app}}$  was calculated by fitting the enzyme inhibition versus compound concentration data using the Morrison equation (equation 9.6 in Copeland<sup>30</sup>) or the competitive inhibition equation (equation 8.1 in Copeland<sup>30</sup>) for less potent inhibitors (see Experimental Section). This approach allows a more accurate determination of affinity for the most highly potent inhibitors approaching the functional limitations of the assay.<sup>31</sup> For SAR interpretation purposes, the  $K_i^{\text{app}}$  values were converted to IC<sub>50</sub> values using the Cheng-Prusoff equation (equation 3 in Cheng and Prusoff<sup>32</sup>) employing an experimentally determined ATP  $K_m$  of 48  $\mu\text{M}$ .<sup>33</sup>

To evaluate intracellular inhibitor potency, a new cell assay was developed. Human full-length ASK1 was over-expressed in HEK293 cells containing a stress-activated luciferase reporter downstream of the

transcription factor Activator Protein-1 (AP-1). AP-1 acts downstream of the stress-activated protein kinase/Jun N-terminal kinase (SAPK/JNK), hence the expectation was that activation of overexpressed ASK1 would lead to a robust reporter cell line for ASK1 kinase activity via MMK4 or MKK7.<sup>7</sup> It was discovered that upon expression, full-length ASK1 was constitutively active in the HEK293/AP-1<sub>luc</sub> cells, and did not require exogenous stimulation for activation, as evidenced by the autophosphorylation of ASK1 at Thr838 (Figure 5, lanes 1 and 2). This basal autophosphorylation was minimally detected in cells overexpressing kinase-inactive ASK1 K709R (Figure 5, lane 3). ASK1 autophosphorylation was blocked by ASK1 selective inhibitors such as **38** dosed at 10  $\mu$ M (Figure 5, lane 4). Despite the constitutive activation of ASK1 in the overexpressing cells, AP-1-induced luciferase expression was not detected in cells. This was supported by the failure to detect phosphorylated JNK (data not shown). Instead, in this cell system, constitutively activated ASK1 resulted in elevated phosphorylation of p38, the other ASK1-dependent substrate via MKK3 and MKK6.<sup>7</sup>

Thus, phosphorylation of p38 was used to measure the intracellular potency of ASK1 inhibitors. In this assay, HEK293/AP-1<sub>luc</sub> cells expressing human full-length ASK1 were incubated with compound for 18 hours and then lysed and the level of phospho-p38 was quantified using the HTRF assay.<sup>33</sup>

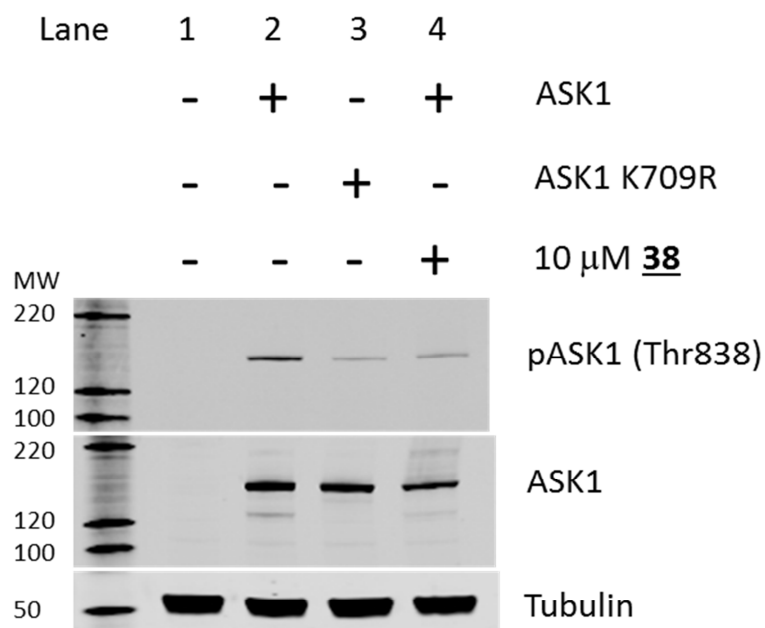


**Figure 6:** Characterization of a cell line overexpressing human full-length ASK1.

Lane 1: HEK293/AP-1<sub>luc</sub> parental cell line; Lane 2: HEK293/AP-1<sub>luc</sub> cells overexpressing full-length ASK1; Lane 3: HEK293/AP-1<sub>luc</sub> cells overexpressing catalytically inactive ASK1 K709R; Lane 4: HEK293/AP-1<sub>luc</sub> cells overexpressing full-length ASK1 treated with **38** (10  $\mu$ M).

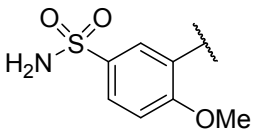
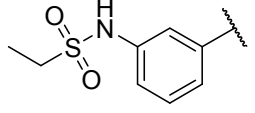
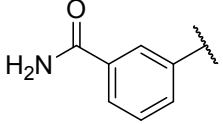
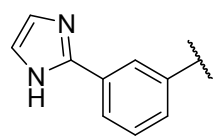
### Results and Discussion

Gratifyingly, several of the 29 prepared library analogs incorporating a variety of chemically diverse substituents were found to display IC<sub>50</sub> values in the recombinant ASK1 enzyme assay below 1  $\mu$ M. Table

1 highlights four key analogs from this initial library with the enzymatic potency, as well as lipophilicity (SFlogD) and lipophilic efficiency (LipE) values shown.<sup>34, 35</sup> Analogs **18** and **25-26** were attractive in that they provided functional groups with synthetically straightforward design opportunities to explore further potency enhancements and adjustment of physicochemical properties. Among the four analogs shown in Table 1, sulfonamide **18** stood out with respect to its enzymatic potency and LipE. This analog is about 30 times more potent than the reversed ethyl sulfonamide **25** which is reflected also in the LipE value of **18** being 2 units higher than that of **25**. Primary sulfonamide **18** was the only analog in the library of 29 compounds which carries a methoxy group in the ortho-position to the amide. It was hypothesized that this substituent led to a significant enhancement in potency as a result of rigidifying the biaryl amide through an intra-molecular hydrogen-bond that lowered the rotational flexibility of the molecule thus bringing the ground state conformation close to the bioactive conformation.

To ascertain whether the o-OMe substituent would consistently lead to a reproducible increase in potency, the methoxy analogs corresponding to reverse sulfonamide **25** and primary amide **26** were prepared and tested for their ability to inhibit ASK1 (Table 2). Indeed, the putative intramolecular hydrogen bond established in analogs **31** and **36** resulted in a >200 fold and >500 fold enzyme potency improvement compared to **25** and **26**, respectively.

**Table 1: Representative analogs of the initial library.**

Compound	R	ASK1 IC <sub>50</sub> (nM) <sup>a</sup>	SFlogD <sup>b</sup>	LipE
<b>18</b>		1.5 ± 0.87	1.3	7.8
<b>25</b>		73 ± 27	1.7	5.7
<b>26</b>		580 ± 130	1.2	5.4
<b>27</b>		170 ± 38	2.4	4.7

<sup>a</sup>Biochemical assay with recombinant human full-length ASK1 in the presence of 1 mM ATP. All results are the mean of at least two independent determinations.

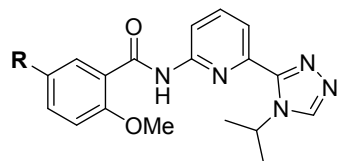
<sup>b</sup> Shake flask logD

It was recognized that the additional hydrogen bond donor substituents on analogs such as **18**, **31** and **36** may have a detrimental effect on permeability. Methyl sulfone **38** was designed to minimize the H-bond donor count while still displaying a functional group that could potentially engage Gln756 as predicted in our docking model. Despite a 3-15 fold reduction in potency in the ASK1 enzyme assay compared to the sulfonamides **18** and **31** as well as amide **36**, the sulfone moiety of inhibitor **38** (IC<sub>50</sub> = 5 nM), remained an attractive functional group to be considered for the design of ASK1 inhibitors as the permeability as measured by RRCK cells (low efflux MDCK cells)<sup>36</sup> was increased.

Overall, the methoxy containing inhibitors are in a desirable lipophilicity range with SFlogD below three<sup>34, 37</sup> (Table 2) as measured in the shake flask logD (SFlogD) assay<sup>38</sup> and have excellent LipE values. These compounds are also characterized by low to moderate molecular weight and acceptable RRCK permeability.<sup>36</sup> As a result of their desirable physicochemical and ADME profile, these analogs were advanced to the cell-based assay described above.

When evaluated in the cellular assay, analogs **18, 31, 36 and 38** are characterized by a significant shift in potency compared to the biochemical enzymatic IC<sub>50</sub> values (Table 2). As indicated above, the kinase assay was carried out in the presence of 1 mM ATP to approximate intracellular ATP concentrations. As a result, a modest enzyme-to-cell shift was expected, especially since the analogs appear to have sufficient cell-permeability as predicted by the measured RRCK values. We postulate that this unexpected shift is due the artificial nature of the engineered cells over expressing ASK1.

**Table 2: Second generation ASK1 inhibitors.**



Compound	R	ASK1 IC50 (nM) <sup>a</sup>	cell IC50 (nM) <sup>b</sup>	SFlogD <sup>c</sup>	LipE	MW	RRCK <sup>d</sup>
<b>18</b>		1.5 ± 0.87	736 ± 272	1.3	7.8	416	2.0
<b>31</b>		0.32 ± 0.12	41 ± 4.2	2.2	7.6	445	5.6
<b>36</b>		1.0 ± 0.46	94 ± 4.5	1.5	7.8	380	3.5
<b>38</b>		5.0 ± 2.9	140 ± 38	1.3	7.3	415	7.9
<b>19</b>		2.4 ± 1.3	272	1.8	7.1	394	9.8

<sup>a</sup> Biochemical assay with recombinant human full-length ASK1 in the presence of 1 mM ATP. All results are the mean of at least two independent determinations.

<sup>b</sup> Human full-length ASK1 over-expressed in HEK293/AP-1luc cells measuring inhibition of p38 phosphorylation. All results are the mean of at least two independent determinations except for compound **19**.

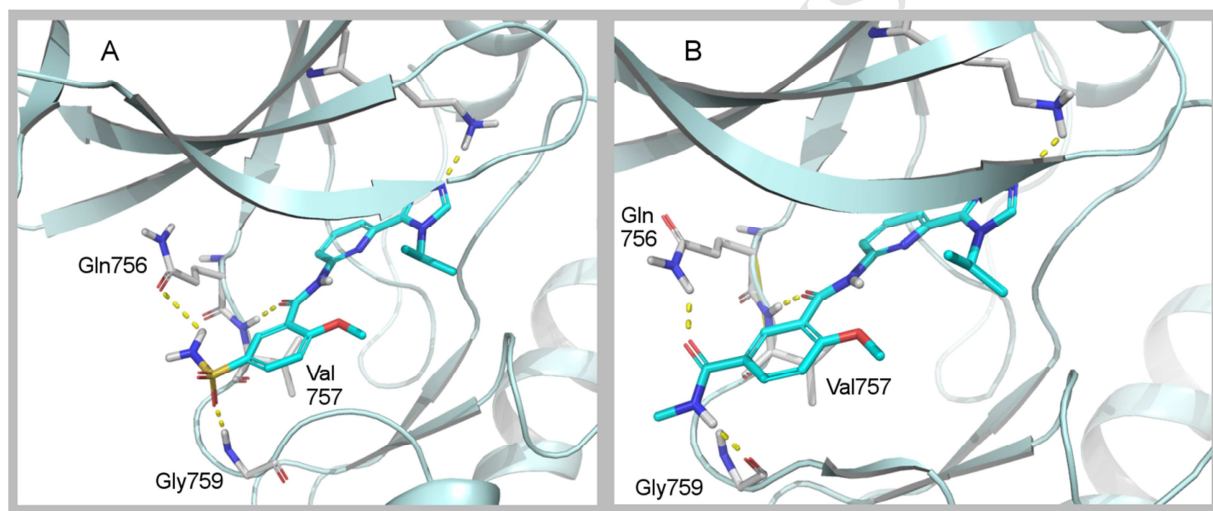
<sup>c</sup> Shake flask log D

<sup>d</sup> (10<sup>-6</sup> cm<sup>2</sup>s<sup>-1</sup>)

To identify compounds with improved enzymatic and cellular potency using structure-based design, several X-ray co-crystal structures of these inhibitors bound in the active site of ASK1 were obtained. To this end, efforts were focused on sulfonamides, amides and sulfones represented by examples **18**, **36** and **38**. The reverse sulfonamide chemotype **31** was deprioritized in order to avoid the potential of forming a reactive p-quinone intermediate under conditions of oxidative metabolism.

Crystal structures were obtained of sulfonamide **18** and amide **19** as a derivative of amide **36** (Figure 7A and B). The precise rotameric orientation of amide **36** was of significant interest to understand the compound's interaction with the protein. As it would be difficult to assign the rotomer of **36**, the N-methyl amide **19** was prepared and utilized for the X-ray crystal structure experiment along with sulfonamide **18**.

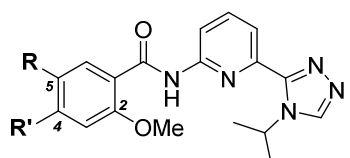
Figure 7 shows the X-ray co-crystal structures for sulfonamide **18** and N-Me amide **19** bound to the ATP-binding site of ASK1. The crystal structures confirmed that the analogs in this series are in fact single-point hinge binders as predicted by our docking model. The amide carbonyl of the inhibitors engages the backbone NH of Val757. As intended, the chemotypes interact with either rotamer of the carboxamide of Gln756 depending on whether a hydrogen bond donor (Figure 7A) or acceptor (Figure 7B) is proximal to the carboxamide side-chain residue. In addition to the Gln756 interaction, the inhibitors also engage Gly759, either through its backbone NH in case of the sulfonamide **18** or through its backbone carbonyl in case of the substituted amide **19**.



**Figure 5:** X-ray co-crystal structures of analogs **18** (A) and **19** (B).

Having confirmed that these ASK1 inhibitors act as single point hinge binders demonstrating the predictive capabilities of the docking model, X-ray protein crystal structure information was used to guide efforts to design more potent inhibitors. As previously described, sulfonamides such as **18** as well as amides such as **19** interact with Gly759. It was hypothesized that the strength of this hydrogen bond could be enhanced by shielding it with a lipophilic substituent on the 4-position of the methoxy-substituted benzamide ring.<sup>39</sup> To test this hypothesis the corresponding 4-methyl analogs of **18**, **36** and

**38** were prepared (Table 3). Improvements in enzyme and cell potencies were observed when comparing sulfonamides **18** with **20** as well as amides **36** with **45**. The potency increased as a result of the addition of the methyl group in the case of the amides **45** and **36** was essentially lipophilic neutral as evidenced by the LipE values of 8.0 vs 7.8. In contrast, sulfonamide **20** benefitted significantly more from the additional methyl substituent beyond the increase in logD: its LipE value improved by a full unit when compared to sulfonamide **18**. This level of potency improvement clearly indicates that the 4-Me group in the context of the sulfonamide substituent has a beneficial impact beyond increasing the lipophilicity. However one must be careful in attributing the cause of the improved activity. Torsion scans of the sulfonamides **18** and **20** and amides **36** and **45** were undertaken using quantum mechanics (QM) as well as molecular mechanics (MM) to assess the effect of the methyl group on the energy of the bound conformation (see Supplementary Materials, Figures SI-2 and SI-3 for corresponding dihedral plots). The torsion scans suggest that the addition of the methyl group ortho to the sulfonamide to afford **20** may have little effect (QM) to a 0.8 kcal stabilization (MM) of the conformational energy. In the case of the amide, ortho methylation is predicted to destabilize the bound conformation by 0.8 kcal (QM) to 0.21 kcal (MM). Thus in the case of the sulfonamides the beneficial effect of the methyl group may not have been compromised by torsion strain, whereas in the case of the amide **45** the conformational effect may have negated any benefit of shielding the H-bond. Sulfone **38** did not benefit from the addition of the methyl group, as sulfone **21** is essentially equipotent to **38** in the enzyme inhibition assay and only shows a twofold improvement in cell potency.

**Table 3: Effect of 4-methyl substitution on ASK1 potency.**


Compound	R	R'	ASK1 IC <sub>50</sub> (nM) <sup>a</sup>	cell IC <sub>50</sub> (nM) <sup>b</sup>	enzyme-to-cell ratio	SFlogD <sup>c</sup>	LipE	MW	RRCK <sup>d</sup>
<b>18</b>		H	1.5 ± 0.87	740 ± 270	490	1.3	7.8	416	2.0
<b>20</b>		Me	0.10 ± 0.12	84 ± 36	840	1.6	8.8	430	2.3
<b>36</b>		H	1.0 ± 0.46	94 ± 4.5	94	1.5	7.8	380	3.5
<b>45</b>		Me	0.42 ± 0.13	28 ± 22	70	1.6	8.0	394	3.5
<b>38</b>		H	5.0 ± 2.9	140 ± 38	28	1.3	7.3	415	7.9
<b>21</b>		Me	4.0 ± 2.7	73 ± 4.2	18	1.7	7.0	429	7.2

<sup>a</sup> Biochemical assay with recombinant human full-length ASK1 in the presence of 1 mM ATP. All results are the mean of at least two independent determinations.

<sup>b</sup> Human full-length ASK1 over-expressed in HEK293/AP-1luc cells measuring inhibition of p38 phosphorylation. All results are the mean of at least two independent determinations.

<sup>c</sup> Shake flask log D

<sup>d</sup> (10<sup>-6</sup> cm<sup>2</sup>s<sup>-1</sup>)

While the additional methyl group in analogs **20** and **45** had a beneficial impact on the enzyme potency of up to 15 fold and cell potency of up to 9 fold it did not have a significant impact on the ratio of enzymatic to cellular IC<sub>50</sub>. The sulfonamides, which are characterized by the lowest permeability as measured by their RRCK values, display the largest shift between the two assays. Conversely, the sulfones, which have the highest permeability, also have the lowest enzyme to cell ratio. In an absolute sense, amide **45** shows the best cell potency among this cohort of ASK1 inhibitors, presumably a composite effect of its enzyme potency and its cell permeability.

At the outset of targeting the two Gln756 side-chain rotamers, it was unclear which rotational isomer would lead to more potent ASK1 inhibitors. While such a preference might have been anticipated, the



colored on a sliding scale wherein zero percent inhibition is green, 50% inhibition is yellow and 100% inhibition is red.

In order to study the pharmacokinetic (PK) profile of this chemotype, compounds **18** and **38** were selected for a rat PK study. Methylsulfone **38** in particular is characterized by the lowest lipophilicity and highest permeability among the ASK1 inhibitors in Table 3 while having low *in vitro* clearance as measured in rat hepatocytes<sup>41</sup> (Table 4). Compound **18** has comparable lipophilicity and *in vitro* clearance but poorer permeability. However, following a 1 mg/kg IV dose, both compounds **18** and **38** were found to have moderate *in vivo* clearance in rat (Table 4, see Supplementary Materials for protocol details). When dosed orally as a solution to minimize kinetic dissolution effects, both compounds **18** and **38** were shown to have low bioavailability (F = 1% and 8% respectively). It may be that though the compounds were dosed as solutions, the low thermodynamic solubility<sup>42</sup> of each compound hindered absorption, but the precise source of the poor bioavailability could not be determined.

**Table 4:** Key *in vitro* and *in vivo* ADME parameters for **18** and **38**.

Compound	<b>18</b>	<b>38</b>
SFlogD (pH 7.4)	1.2	1.3
thermodynamic solubility pH 7.4 ( $\mu\text{M}$ )	1.2	5
RRCK ( $10^{-6} \text{ cm}\cdot\text{s}^{-1}$ )	2.04	7.9
rat hepatocyte Cl ( $\text{mL}\cdot\text{min}^{-1}\cdot 10^{-6} \text{ cells}$ )	< 6	<6
rat IV Cl ( $\text{mL}\cdot\text{min}^{-1}\cdot\text{kg}^{-1}$ )	35	41
rat F (mg/kg)	< 1% (5)	8% (1)

## Conclusions

A careful analysis of the ATP-binding site of ASK1 was carried out which identified the relatively unique Gln756 position and thus provided an intriguing design hypothesis for the identification of selective ASK1 inhibitors. An investigation of how compound **4** binds to ASK1 led to the hypothesis that it is a single point hinge binder via the carbonyl oxygen. This binding hypothesis was later validated by protein crystallography. This hypothesis informed the design of a virtual library of ~14K amides which was enumerated *in silico* and triaged based on the analogs' ability to engage either one of the two rotamers of the Gln756 amide side chain. Several of the 29 amides targeted for synthesis were found to have IC<sub>50</sub> values below 1 μM when tested in the full-length ASK1 biochemical kinase assay in the presence of 1 mM ATP as exemplified by amide **18** with an IC<sub>50</sub> of 2 nM and LipE of 7.8. Subsequent SAR work led to the discovery of a series of sulfonamides, amides and sulfones with sub-nanomolar potencies when assayed against the ASK1 enzyme. In addition to displaying attractive enzymatic activity, several analogs were found to be highly potent in a cell-based assay measuring inhibition of phosphorylation of p38, a key kinase downstream of ASK1 involved in the regulation of inflammation and oncology pathways. Though potent in the cell-based assay, there was a large right shift between enzyme and cellular potency potentially due to the limited cell permeability as predicted by the low RRCK and over expression of ASK1 in HEK293 cells. In addition to excellent potency, these inhibitors deliver a high degree of kinome selectivity when assessed in a panel of 40 kinases. While lead compounds from this program displayed encouraging *in vitro* ADME properties oral bioavailability in rat was poor. Further efforts will have to be undertaken to address the series' low bioavailability (as exemplified by compounds **18** and **38**). However, the ASK1 inhibitors reported here constitute attractive tool compounds with the potential to support the elucidation of the pharmacological consequences of ASK1 inhibition.

## Experimental section

### **Synthesis information**

#### **General Methods**

Unless specified, all solvent were purchased as anhydrous sealed bottles and used as received. Standard techniques for handling air-sensitive compounds were employed for indicated operations. Removal of solvents was accomplished on a rotary evaporator at reduced pressure. The purity of compounds of the final compounds **18-21, 25-27, 31, 36, 38 and 45** was determined by either HPLC or UPLC analysis and determined to be >95% pure.

Low-Resolution Mass Spectrometry analyses were conducted on Waters Acquity UPLC (Acquity Binary Solvent Manager, 2777C-Autosampler, Acquity PDA, Acquity ELS and Acquity Column Manager) and Waters Acquity SQ systems from Waters Corporation, Milford, MA. Signal acquisition conditions included: Waters Acquity HSS T3, 2.1mmx50mm, C18, 1.7 $\mu$ m; Column Temperature 60 °C as the column; 0.1% formic acid in water (v/v) as the mobile phase A; 0.1% formic acid in acetonitrile (v/v) as the mobile phase B; 1.25mL/min as the flow and ESCI (ESI+/-, APCI+/-), 100-2000m/z scan, 0.4sec scan time, Centroid as the MS method.

High-Resolution Mass Spectrometry analyses were conducted on an Agilent 6220 TOF mass spectrometer (Agilent Technologies, Wilmington, DE) in positive or negative electrospray mode. The system was calibrated to greater than 1ppm accuracy across the mass range prior to analyses according to manufacturer's specifications. The samples were separated using UHPLC on an Agilent 1200 (Agilent Technologies, Wilmington, DE) system prior to mass spectrometric analysis. The resulting spectra were automatically lockmass corrected and the target mass ions and any confirming adducts (Na<sup>+</sup>, NH<sub>4</sub><sup>+</sup>) were extracted and combined as a chromatogram. The mass accuracy was calculated for all observed isotopes against the theoretical mass ions derived from the chemical formula using MassHunter software (Agilent Technologies, Wilmington, DE).

All NMR spectra were collected on either a Bruker 400 Avance III with a 5 mm BBFO probe (400 MHz for <sup>1</sup>H; 101 MHz for <sup>13</sup>C) or a Bruker 500 Avance III HD with a 5 mm BBO Nitrogen cryoprobe (500 MHz for <sup>1</sup>H; 126 MHz for <sup>13</sup>C). The proton signal for non-deuterated solvent ( $\delta$  7.27 for CHCl<sub>3</sub>,  $\delta$  2.50 for DMSO,  $\delta$  3.31 for MeOH) was used as an internal reference for <sup>1</sup>H NMR spectra. For <sup>13</sup>C NMR spectra, chemical shifts are reported relative to the  $\delta$

77.00 resonance of  $\text{CDCl}_3$  or  $\delta$  39.51 resonance of  $\text{DMSO-d}_6$ . Deuterated solvents ( $\text{CDCl}_3$ ,  $\text{CD}_3\text{OD}$  and  $\text{DMSO-d}_6$ ) were purchased from Cambridge Isotope Laboratories Inc. and used as received.

ACCEPTED MANUSCRIPT

## Procedures

*2-methoxy-N-[6-[4-(propan-2-yl)-4H-1,2,4-triazol-3-yl]pyridin-2-yl]-5-sulfamoylbenzamide (18)*. To a mixture of 2-methoxy-5-sulfamoylbenzoic acid (**17**, 500.0 mg, 2.16 mmol) in acetonitrile (10.0 mL) was added DMF (90 mg, 1 mmol, 0.1 mL) followed by oxalyl chloride (297 mg, 2.27 mmol, 0.204 mL). The mixture was stirred at ambient temperature under nitrogen for 1 h. In a separate flask a mixture of 6-[4-(propan-2-yl)-4H-1,2,4-triazol-3-yl]pyridin-2-amine<sup>25</sup> (440 mg, 2.16 mmol) and pyridine (3.0 mL, c=0.2 M) was stirred at ambient temperature. After 1 h the slurry of the amine in pyridine was added to the acid chloride reaction resulting in a clear yellow solution. The mixture was stirred under nitrogen at ambient temperature for 4.5 h, at which point it became a slurry. The solids were filtered, washed with acetonitrile and dried under vacuum to give a crude amorphous material. In an open flask, the solids (~400 mg) were refluxed in ethanol (450 mL) and water (20 mL) until the volume reached ~ 100 mL. Further ethanol (300 mL) was added and the operation was repeated until a volume of ~ 50 mL. The mixture was then allowed to slowly cool down to ambient temperature overnight, and the resulting crystalline solids were filtered and dried under vacuum to provide the title compound (384 mg, 43%). <sup>1</sup>H NMR (400 MHz, DMSO-d<sub>6</sub>): δ 10.69 (s, 1H), 8.89 (s, 1H), 8.29 (d, J=8.2 Hz, 1H), 8.26 (d, J=2.3 Hz, 1H), 8.05 (t, J=8.0 Hz, 1H), 8.01 - 7.96 (m, 1H), 7.90 (d, J=7.4 Hz, 1H), 7.43 (d, J=8.6 Hz, 1H), 7.38 (s, 2H), 5.56 (td, J=6.6, 13.3 Hz, 1H), 4.02 (s, 3H), 1.50 (d, J=6.6 Hz, 6H). <sup>13</sup>C NMR (500 Mhz, DMSO-d<sub>6</sub>): δ 163.77, 159.56, 151.20, 146.72, 143.81, 140.40, 137.11, 131.00, 128.70, 123.60, 119.75, 114.61, 113.39, 57.33, 48.64, 23.67 MS m/z 417 [M+H]<sup>+</sup>

*3-(ethylsulfonamido)-N-(6-(4-isopropyl-4H-1,2,4-triazol-3-yl)pyridin-2-yl)benzamide (25)*. To a solution of 3-(ethylsulfonamido)benzoic acid (**22**, 60 μmol) and 6-[4-(propan-2-yl)-4H-1,2,4-triazol-3-yl]pyridin-2-amine (**5**, 50 μmol) in EtOAc (1 mL) was added T<sub>3</sub>P (50% in EtOAc, 1 mL) and triethylamine (207 μmol). The vial was placed under a positive atmosphere of nitrogen, capped and shaken at 100 °C for 16 h. The reaction was concentrated under reduced pressure and purified by HPLC ( Phenomenex Gemini C18 250×21.2mm\*8μm; Acetonitrile-NH<sub>4</sub>OH (pH 10); gradient from 0% to 40% in 8 minutes, flow rate 35 mL/min). MS m/z 415 [M+H]<sup>+</sup>

*N-[6-[4-(propan-2-yl)-4H-1,2,4-triazol-3-yl]pyridin-2-yl]benzene-1,3-dicarboxamide (26)* Compound 26 was prepared following the procedure for compound 25 using 3-(aminocarbonyl) benzoic acid (**23**) and was purified by

HPLC (Phenomenex Gemini C18 250×21.2mm\*8μm; Acetonitrile-NH<sub>4</sub>OH (pH 10); gradient from 19% to 59% in 8 minutes, flow rate 35 mL/min). MS m/z 351 [M+H]<sup>+</sup>

3-(1*H*-imidazol-2-yl)-*N*-(6-[4-(propan-2-yl)-4*H*-1,2,4-triazol-3-yl]pyridin-2-yl)benzamide (**27**). Compound **27** was prepared following the procedure for compound **25** using 3-(1*H*-imidazol-2-yl) benzoic acid (**24**) and was purified by HPLC (Phenomenex Gemini C18 250×21.2mm\*8μm; Acetonitrile-NH<sub>4</sub>OH (pH 10); gradient from 3% to 43% in 8 minutes, flow rate 35 mL/min). MS m/z 374 [M+H]<sup>+</sup>

methyl 5-(ethylsulfonamido)-2-methoxybenzoate (**29**). To a solution of ethyl 5-amino-2-methoxybenzoate (**28**, 1.2 g, 6.147 mmol) in DCM (20 mL) was added pyridine (1.46 g, 18.4 mmol) and ethanesulfonyl chloride (948 mg, 7.38 mmol). The mixture was stirred at 20 °C for 2 h. The mixture was diluted with DCM (200 mL), washed with a 1N HCl solution (50 mL) and then saturated aqueous NaHCO<sub>3</sub> (100 mL), dried over Na<sub>2</sub>SO<sub>4</sub> and concentrated under reduced pressure. The title compound (1.7 g, 96%) was obtained as a brown oil. <sup>1</sup>H NMR (400 MHz, CDCl<sub>3</sub>): δ 7.65 (d, J=3.0 Hz, 1H), 7.46 (dd, J=2.8, 8.8 Hz, 1H), 6.95 (d, J=9.0 Hz, 1H), 6.94 (br. s, 1H), 4.36 (q, J=7.0 Hz, 2H), 3.88 (s, 3H), 3.08 (q, J=7.5 Hz, 2H), 1.37 (t, J=7.0 Hz, 2H). MS m/z 296 [M+Na]<sup>+</sup>.

5-(ethylsulfonamido)-2-methoxybenzoic acid (**30**). To a solution of ethyl 5-[(ethylsulfonyl)amino]-2-methoxybenzoate (**29**, 1.7 g, 5.92 mmol) in THF/ water (1:1, 16 mL) was added NaOH (710 mg, 17.7 mmol). The mixture was stirred at 20 °C for 4 h. THF was removed under reduced pressure. The mixture was adjusted to pH=3 by addition of a 1N HCl solution. A precipitate formed and was filtered off to afford the title compound (1.2 g, 78%) as an off-white solid. <sup>1</sup>H NMR (400MHz, DMSO-d<sub>6</sub>): δ 9.60 (s, 1H), 7.49 (d, J=3.0 Hz, 1H), 7.34 (dd, J=3.0, 8.5 Hz, 1H), 7.10 (d, J=8.5 Hz, 1H), 3.78 (s, 3H), 3.00 (q, J=7.0 Hz, 2H), 1.18 (t, J=7.0 Hz, 3H). MS m/z 282 [M+Na]<sup>+</sup>.

5-(ethylsulfonamido)-*N*-(6-(4-isopropyl-4*H*-1,2,4-triazol-3-yl)pyridin-2-yl)-2-methoxybenzamide (**31**). To a suspension of 5-[(ethylsulfonyl)amino]-2-methoxybenzoic acid (**30** 1.2 g, 4.63 mmol) in acetonitrile (10 mL) was added SOCl<sub>2</sub> (578 mg, 4.86 mmol). The mixture was stirred at 50 °C for 1 hour. The solvent and excess SOCl<sub>2</sub> were removed under reduced pressure to give the crude acid chloride as an off-white solid, which was used directly for the next step. To a solution of this crude material (1.29 g, 4.645 mmol) in acetonitrile (10 mL) was added a solution of 6-[4-(propan-2-yl)-4*H*-1,2,4-triazol-3-yl]pyridin-2-amine (**5**, 944 mg, 4.64 mmol) in acetonitrile (8 mL). The mixture was stirred at 20 °C for 1 hour. A precipitate formed and was filtered then recrystallized from MeOH (80 mL). The solid was dried under high vacuum at 50 °C for 16 hours to afford the title compound (684 mg, 33%) as an

off-white solid.  $^1\text{H}$  NMR (400 MHz, DMSO- $d_6$ ):  $\delta$  10.71 (s, 1H), 9.79 (s, 1H), 9.58 (s, 1H), 8.37 (d,  $J=8.0$  Hz, 1H), 8.10 (t,  $J=7.8$  Hz, 1H), 7.92 (d,  $J=7.5$  Hz, 1H), 7.75 (d,  $J=2.5$  Hz, 1H), 7.45 (dd,  $J=2.8, 8.8$  Hz, 1H), 7.27 (d,  $J=9.0$  Hz, 1H), 5.62 (spt,  $J=6.3$  Hz, 1H), 3.95 (s, 3H), 3.05 (q,  $J=7.0$  Hz, 2H), 1.55 (d,  $J=6.5$  Hz, 6H), 1.21 (t,  $J=7.3$  Hz, 3H).  $^{13}\text{C}$  NMR (500 Mhz, DMSO- $d_6$ ): 154.31, 151.42, 150.15, 147.5, 143.81, 140.61, 132.08, 126.29, 123.36, 123.21, 120.01, 114.15, 57.06, 45.35, 23.47, 8.45. MS  $m/z$  445  $[\text{M}+\text{H}]^+$ .

*methyl 5-cyano-2-methoxybenzoate (33)*. A solution of 3-bromo-4-methoxybenzotrile (**32**, 1 g, 4.72 mmol), triethylamine (954 mg, 9.43 mmol) and Pd(dppf) $\text{Cl}_2$  (150 mg, 0.205 mmol) in MeOH (20 mL) was stirred at 100 °C under CO atmosphere (60 psi) for 4 hours. The reaction mixture was then cooled down, concentrated under reduced pressure and the resulting crude material was purified by column chromatography on silica gel (PE/EtOAc=100/0-80/20) The title compound (200 mg, 22%) was obtained as a white solid.  $^1\text{H}$  NMR (400 MHz,  $\text{CDCl}_3$ ):  $\delta$  8.11 (d,  $J=2.0$  Hz, 1H), 7.76 (dd,  $J=2.0, 8.5$  Hz, 1H), 7.06 (d,  $J=9.0$  Hz, 1H), 3.98 (s, 3H), 3.92 (s, 3H). MS  $m/z$  192  $[\text{M}+\text{H}]^+$ .

*5-cyano-2-methoxybenzoic acid (34)*. To a solution of methyl 5-cyano-2-methoxybenzoate (**33**, 200 mg, 1.05 mmol) in THF/ water (4 mL, 1:1) was added LiOH $\cdot\text{H}_2\text{O}$  (110 mg, 2.62 mmol). The mixture was stirred at 20 °C for 4 hours. THF was then removed and the mixture was adjusted to pH=2 with a 2N HCl solution. A precipitate formed and was filtered, then dried to afford the title compound (150 mg, 81%) as an off-white solid.  $^1\text{H}$  NMR (400 MHz, DMSO- $d_6$ ):  $\delta$  13.14 (br. s., 1H), 8.01 (d,  $J=2.0$  Hz, 1H), 7.97 (dd,  $J=2.0, 8.5$  Hz, 1H), 7.31 (d,  $J=8.5$  Hz, 1H), 3.90 (s, 3H). MS  $m/z$  178  $[\text{M}+\text{H}]^+$ .

*5-cyano-N-(6-(4-isopropyl-4H-1,2,4-triazol-3-yl)pyridin-2-yl)-2-methoxybenzamide (35)*. To a solution of 5-cyano-2-methoxybenzoic acid (**34**, 130 mg, 0.734 mmol), 6-[4-(propan-2-yl)-4H-1,2,4-triazol-3-yl]pyridin-2-amine (149 mg, 0.734 mmol) and diisopropylethylamine (379 mg, 2.94 mmol) in THF (5 mL) was added Mukaiyama's reagent<sup>29</sup> (281 mg, 1.10 mmol). The mixture was stirred at 70 °C for 4 hours. The mixture was cooled down to room temperature and diluted with DCM (100 mL). The organic layer was washed with brine (100 mL), water (100 mL), dried over  $\text{Na}_2\text{SO}_4$  and concentrated under reduced pressure to give the title product (260 mg), which was used directly for the next step without further purification. MS  $m/z$  363  $[\text{M}+\text{H}]^+$ .

*N1-(6-(4-isopropyl-4H-1,2,4-triazol-3-yl)pyridin-2-yl)-6-methoxyisophthalamide (36)*: To a solution of 5-cyano-2-methoxy-N-{6-[4-(propan-2-yl)-4H-1,2,4-triazol-3-yl]pyridin-2-yl}benzamide (**35**, 260 mg, crude) in DMSO (4 mL) was added  $\text{K}_2\text{CO}_3$  (496 mg, 3.59 mmol) and  $\text{H}_2\text{O}_2$  (171 mg, 5.02 mmol) at 0 °C. The mixture was

stirred at 20 °C for 30 minutes. The mixture was diluted with DCM (100 mL), washed with brine (100 mL), water (100 mL), dried over Na<sub>2</sub>SO<sub>4</sub> and concentrated under reduced pressure. The crude product was purified by preparative HPLC (DuraShell 150\*25mm\*5μm; gradient from 18% to 38% MeCN in water (0.225% FA) in 11 minutes, flow rate: 25 mL/min.) to afford the title compound (28 mg, 10% for 2 steps) as an off-white solid. <sup>1</sup>H NMR (400 MHz, DMSO-d<sub>6</sub>): δ 10.67 (s, 1H), 8.89 (s, 1H), 8.36 (d, J=2.0 Hz, 1H), 8.31 (d, J=8.5 Hz, 1H), 8.09 (dd, J=2.3, 8.8 Hz, 1H), 8.06 - 8.01 (m, 2H), 7.89 (d, J=7.5 Hz, 1H), 7.34 (br. s., 1H), 7.32 (d, J=8.5 Hz, 1H), 5.57 (sept, J=6.4 Hz, 1H), 4.00 (s, 3H), 1.49 (d, J=7.0 Hz, 6H). <sup>13</sup>C NMR (500 Mhz, DMSO-d<sub>6</sub>): 167.74, 164.48, 159.46, 151.38, 150.20, 146.69, 143.79, 140.32, 132.85, 130.53, 127.25, 123.18, 119.57, 114.49, 112.60, 57.03, 48.61, 23.67. MS m/z 381 [M+H]<sup>+</sup>.

*2-methoxy-5-(methylsulfonyl)-N-{6-[4-(propan-2-yl)-4H-1,2,4-triazol-3-yl]pyridin-2-yl}benzamide (38)*. 2-Methoxy-5-(methylsulfonyl)benzoic acid (**37**, 691mg, 3 mmol) was suspended in SOCl<sub>2</sub> (15mL). The mixture was heated at 55 °C for 1 hour. The mixture was then cooled to room temperature and concentrated under vacuum to afford the acid chloride intermediate (720 mg, 100%) as a white solid which was used in next step without further purification. This crude material and 6-[4-(propan-2-yl)-4H-1,2,4-triazol-3-yl]pyridin-2-amine (**5**, 488 mg, 2.4 mmol) were dissolved in pyridine (10 mL). The mixture was stirred at room temperature for 2 hours. The mixture was then concentrated under reduced pressure. The residue was heated in a 1N NaOH solution (10 mL) at 60 °C for 10 minutes. The heterogeneous mixture was filtered and the cake was washed with a 1N NaOH solution (2\*10mL). The filtrate was acidified by a 6N HCl solution until pH=5. The resulting solid was filtered and washed with water (2\*10mL). Then the solid was heated in iso-propanol (100 mL) at 80 °C for 1 hour. The mixture was filtrated while hot and the filtrate was heated in iso-propanol for 1 hour until the solution became clear. The mixture was then cooled to room temperature overnight. The precipitate that formed was filtered, washed with cold iso-propanol (5 mL), and dried under vacuum to afford the title compound (436 mg, 35%) as a white solid. <sup>1</sup>H NMR (400 MHz, DMSO-d<sub>6</sub>): δ 10.73 (s, 1H), 8.88 (s, 1H), 8.28 (d, J=8.0 Hz, 1H), 8.25 (d, J=2.5 Hz, 1H), 8.09 (dd, J=2.5, 9.0 Hz, 1H), 8.05 (t, J=8.0 Hz, 1H), 7.90 (d, J=7.5 Hz, 1H), 7.49 (d, J=8.5 Hz, 1H), 5.58 (sept, J=6.7 Hz, 1H), 4.03 (s, 3H), 3.24 (s, 3H), 1.48 (d, J=6.5 Hz, 6H). <sup>13</sup>C NMR (500 Mhz, DMSO-d<sub>6</sub>): 163.75, 160.88, 151.02, 150.17, 146.72, 143.78, 140.35, 133.39, 132.33, 129.81, 124.62, 119.75, 114.63, 113.75, 57.43, 48.58, 44.28, 23.67

. MS m/z 416 [M+H]<sup>+</sup>. HRMS for C<sub>19</sub>H<sub>22</sub>N<sub>5</sub>O<sub>4</sub>S [M+H]<sup>+</sup>: calc. 416.1387, exp. 416.1384.

*3-bromo-4-methoxy-N-methylbenzamide (7)*: To a solution of 3-bromo-4-methoxybenzoic acid (**6**, 1000 mg, 4.33 mmol) in dry DCM (30 mL) was added MeNH<sub>2</sub>·HCl (584 mg, 8.66 mmol) and diisopropylamine (2240 mg, 17.3 mmol), followed by EDCI (1330 mg, 6.93 mmol) and HOBt (994 mg, 7.36 mmol). The pale yellow slurry was stirred for 18 hours at room temperature. The solution was then concentrated under reduced pressure and the residue was taken up in EtOAc (50 mL). The organic phase was washed with water (3\*20 mL), dried over Na<sub>2</sub>SO<sub>4</sub>, filtered, and concentrated to dryness to afford the title compound (1.29g, >100%) as a white solid. The latter was used directly in the following step without further purification. <sup>1</sup>H NMR (400 MHz, CDCl<sub>3</sub>): δ 7.94 (d, J=2.0 Hz, 1H), 7.71 (dd, J=2.0, 8.5 Hz, 1H), 6.90 (d, J=8.5 Hz, 1H), 6.47 (br. s., 1H), 3.93 (s, 3H), 2.99 (d, J=5.0 Hz, 3H). MS m/z 246 [M+H]<sup>+</sup>.

*methyl 2-methoxy-5-(methylcarbamoyl)benzoate (8)*. To a solution of 3-bromo-4-methoxy-N-methylbenzamide (**7**, 600 mg, 2.46 mmol), triethylamine (0.497 g, 4.92mmol), Pd(OAc)<sub>2</sub> (55.2 mg, 0.246 mmol) and 1,3-bis(diphenylphosphino)propane (101 mg, 0.246 mmol) in DMF (15 mL) was added MeOH (15 mL). The mixture was stirred at 80 °C under CO atmosphere (50 psi) for 16 hours. LCMS showed the starting material was consumed completely and the desired compound was formed. The reaction mixture was filtered through celite and the filtrate was diluted with EtOAc (50 mL). The organic phase was washed with brine (3\*20 mL), dried over Na<sub>2</sub>SO<sub>4</sub>, filtered, and concentrated under reduced pressure. The residue was purified by flash column chromatography on silica gel (EtOAc in petroleum ether, from 50%-100%) to afford the title compound (500 mg, 91%) as a white solid. <sup>1</sup>H NMR (400 MHz, CDCl<sub>3</sub>): δ 8.20 (d, J=2.5 Hz, 1H), 8.01 (dd, J=2.3, 8.8 Hz, 1H), 7.03 (d, J=9.0 Hz, 1H), 6.26 (br. s., 1H), 3.96 (s, 3H), 3.91 (s, 3H), 3.02 (d, J=5.0 Hz, 3H). MS m/z 224 [M+H]<sup>+</sup>.

*2-methoxy-5-(methylcarbamoyl)benzoic acid (9)*. To a solution of methyl 2-methoxy-5-(methylcarbamoyl)benzoate (**8**, 500 mg, 2.24 mmol) in a mixed solvent of methanol (10 mL) and water (10 mL) was added LiOH (107 mg, 4.48 mmol). The pale yellow slurry was stirred at room temperature for 1 hour. The reaction mixture was then acidified with 1N HCl until pH=5. Solvents were removed under reduced pressure and the title compound was obtained by lyophilization (365 mg, 78%) as a white solid. <sup>1</sup>H NMR (400 MHz, D<sub>2</sub>O): δ 7.89 (m, 1H), 7.51 (m, 1H), 7.17 (m, 1H), 3.93 (s, 3H), 2.88 (s, 3H). MS m/z 210 [M+H]<sup>+</sup>.

*4-methoxy-N-1-methyl-N-3-~{6-[4-(propan-2-yl)-4H-1,2,4-triazol-3-yl]pyridin-2-yl}benzene-1,3-dicarboxamide*

**(19)**. To a stirred solution of 2-methoxy-5-(methylcarbamoyl)benzoic acid (**9**, 90.0 mg, 0.40 mmol) in CH<sub>3</sub>CN (3mL) was added DMF (17.7 mg, 0.242 mmol) and oxalyl chloride (53.7 mg, 0.423 mmol). The mixture was stirred at room temperature for 1 hour. To the resulting solution was added 6-[4-(propan-2-yl)-4H-1,2,4-triazol-3-yl]pyridin-2-amine (**5**, 87.4 mg, 0.430 mmol) in portions. After about 5 minutes some precipitate formed. The reaction mixture was stirred at room temperature for 16 hours. The precipitate was collected by filtration, washed with MeCN (2\*2 mL), dried under vacuum to afford the title compound (10.6 mg, 6%) as a white solid. <sup>1</sup>H NMR (400 MHz, DMSO-d<sub>6</sub>): δ 10.70 (s, 1H), 9.18 (s, 1H), 8.53 (br. d, J=4.0 Hz, 1H), 8.37 - 8.30 (m, 2H), 8.10 - 8.04 (m, 2H), 7.90 (d, J=7.5 Hz, 1H), 7.33 (d, J=9.0 Hz, 1H), 5.61 (spt, J=6.3 Hz, 1H), 3.99 (s, 3H), 2.78 (d, J=4.5 Hz, 3H), 1.51 (d, J=6.5 Hz, 6H). <sup>13</sup>C NMR (500 Mhz, DMSO-d<sub>6</sub>): 165.82, 164.38, 159.32, 151.65, 150.20, 146.70, 143.79, 140.34, 132.46, 130.04, 127.47, 123.05, 119.58, 114.48, 112.72, 57.04, 48.62, 26.74, 23.67. MS m/z 395 [M+H]<sup>+</sup>.

*5-(chlorosulfonyl)-2-methoxy-4-methylbenzoic acid (11)*. To a 100-mL 3-necked flask was added ClSO<sub>3</sub>H (8.41 g, 72.17 mmol) and DCM (3 mL) followed by SOCl<sub>2</sub> (2.58 g, 21.69 mmol). The flask was fitted with a basic scrub using Drechsel bottle containing a 1M NaOH solution. The mixture was cooled to -5 °C using a dry ice-acetone bath. 2-Methoxy-4-methylbenzoic acid (**10**, 3.0 g, 18 mmol) was added in portions. The reaction temperature was maintained below 5 °C over this time. The cold bath was removed and the reaction mixture allowed to warm to 20 °C for 5 hours. The reaction was cautiously quenched into a beaker containing 20 g of ice which was placed in an ice-bath, over a period of 10 minutes. The temperature of the mixture in the beaker should not exceed 5 °C. The ice bath was removed and the mixture was stirred for 5 minutes before filtering off the resulting white solid which was washed with water and dried in vacuo to afford the title compound (2.9 g, 61%) as a white solid. <sup>1</sup>H NMR (400 MHz, DMSO-d<sub>6</sub>): δ 13.81 (br. s., 1H), 8.07 (s, 1H), 6.90 (s, 1H), 3.80 (s, 3H), 2.55 (s, 3H). MS m/z 265 [M+H]<sup>+</sup>.

*2-methoxy-4-methyl-5-sulfamoylbenzoic acid (12)*: 5-(Chlorosulfonyl)-2-methoxy-4-methylbenzoic acid (**11**, 25 mg, 0.094 mmol) was dissolved in portions in 25% aq. NH<sub>3</sub> (2 ml) at 0 °C. After 5 minutes, LCMS showed the reaction was complete. The solvent was evaporated and the residue dissolved in water (3 mL). Conc. HCl was added until pH 2 and the white precipitate that formed was filtered, washed with water (3 x 2 mL) and dried to afford the title compound (10 mg, 43%) as a white solid. <sup>1</sup>H NMR (400 MHz, DMSO-d<sub>6</sub>): δ 12.83 (brs, 1H), 8.18 (s, 1H), 7.36 (s, 2H), 7.14 (s, 1H), 3.88 (s, 3H), 2.62 (s, 3H). MS m/z 246 [M+H]<sup>+</sup>.

*2-Methoxy-5-(methylsulfamoyl)-N-{6-[4-(propan-2-yl)-4H-1,2,4-triazol-3-yl]pyridin-2-yl}benzamide (20)*. To a solution of 5-(chlorosulfonyl)-2-methoxy-4-methylbenzoic acid (**12**, 40 mg, 0.16 mmol) in acetonitrile (3 mL) was added DMF (11.9 mg, 0.163 mmol) and oxalyl chloride (51 mg, 0.40 mmol). The reaction mixture was stirred at 20 °C for 1 h. Then 6-[4-(propan-2-yl)-4H-1,2,4-triazol-3-yl]pyridin-2-amine (**5**, 32.5 mg, 0.160 mmol) and pyridine (31.6 mg, 0.400 mol) were added at 0 °C. The reaction mixture was stirred at 20 °C for 4 h. Ethyl acetate (30 mL) was added into the reaction mixture and the organic layer was washed with saturated aqueous NaHCO<sub>3</sub> solution (10 mL). Some solids crashed out of the solution and were collected. The organic solvent was dried over Na<sub>2</sub>SO<sub>4</sub>, filtered and evaporated under reduced pressure. The residue and the solid were triturated and rinsed with EtOAc to afford the title compound (30 mg, 43%) as a white solid. <sup>1</sup>H NMR (400 MHz, DMSO-d<sub>6</sub>): δ 10.56 (br. s., 1H), 8.90 (s, 1H), 8.39 (s, 1H), 8.30 (d, J=8.0 Hz, 1H), 8.04 (t, J=7.8 Hz, 1H), 7.88 (d, J=7.5 Hz, 1H), 7.44 (br. s., 2H), 7.30 (s, 1H), 5.58 - 5.44 (m, 1H), 4.04 (s, 3H), 2.67 (s, 3H), 1.52 (d, J=6.5 Hz, 6H). MS m/z 431 [M+H]<sup>+</sup>.

*methyl 5-bromo-2-hydroxy-4-methylbenzoate (40)*: Bromine (0.47 ml, 9.03 mmol) was added dropwise to a solution of methyl 2-hydroxy-4-methylbenzoate (**39**, 500 mg, 3.01 mmol) in chloroform (20 mL) at 0 °C. The solution was stirred for 3 h at 0 °C. Then the reaction was quenched with saturated sodium sulphite (5 mL), extracted with dichloromethane (2\*10 mL). The combined organic layers were washed with brine (10 mL), dried over MgSO<sub>4</sub> and the solvent was removed under reduced pressure to afford the title compound (700 mg, 95%) as a white solid. <sup>1</sup>H NMR (400 MHz, CDCl<sub>3</sub>): δ 10.59 (s, 1H), 7.97 (s, 1H), 6.89 (s, 1H), 3.95 (s, 3H), 2.39 (s, 3H).

*methyl 5-bromo-2-methoxy-4-methylbenzoate (41)*: To a mixture of methyl 5-bromo-2-hydroxy-4-methylbenzoate (**40**, 2.9 g, 11.83 mmol) and K<sub>2</sub>CO<sub>3</sub> (3.27 g, 23.7 mmol) in anhydrous acetonitrile (25 mL) was added MeI (2.52 g, 17.8 mmol). The mixture was stirred at 40 °C for 2 h and then at room temperature overnight (16 h). The mixture was then evaporated to dryness and the residue was taken up in EtOAc (50 mL) and water (30 mL), then the aqueous phase was separated. The organic layer was washed with brine (2\*20 mL), dried over Na<sub>2</sub>SO<sub>4</sub>, filtered, concentrated to dryness to give the crude material which was purified by flash column chromatography on silica gel (EtOAc in petroleum ether, 0%-20%) afforded the title compound (526 mg, 17%) as a crystalline white solid. <sup>1</sup>H NMR (400 MHz, CDCl<sub>3</sub>): δ 7.97 (s, 1H), 6.85 (s, 1H), 3.89 (s, 3H), 3.88 (s, 3H), 2.43 (s, 3H). MS m/z 259 [M+H]<sup>+</sup>.

*methyl 5-cyano-2-methoxy-4-methylbenzoate (42)*: A mixture of methyl 5-bromo-2-methoxy-4-methylbenzoate (**41**, 100 mg, 0.39 mmol), Zn(CN)<sub>2</sub> (31.7 mg, 0.27 mmol), xantphos (2.23 mg, 0.0039 mmol), Pd<sub>2</sub>(dba)<sub>3</sub> (21.2 mg, 0.0232

mmol) and N,N,N',N'-tetramethylethylenediamine (8.97 mg, 0.0772 mmol) in anhydrous DMF (1 mL) was placed in a 5 mL tube. Nitrogen was bubbled through the mixture for 5 min, then the tube was immediately sealed and heated to 160 °C (under microwave irradiations) for 200 seconds. The mixture was then cooled down to room temperature and diluted with EtOAc (30 mL). The organic phase was washed with brine (3\*10 mL), dried over Na<sub>2</sub>SO<sub>4</sub>, filtered, and concentrated under reduced pressure. The crude was purified by flash column chromatography on silica gel (EtOAc in petroleum ether, 0%-50%) to afford the title compound (73 mg, 92%) as a white solid. <sup>1</sup>H NMR (400 MHz, CDCl<sub>3</sub>): δ 8.09 (s, 1H), 6.89 (s, 1H), 3.97 (s, 3H), 3.90 (s, 3H), 2.59 (s, 3H). MS m/z 206 [M+H]<sup>+</sup>.

*5-cyano-2-methoxy-4-methylbenzoic acid (43)*. To a mixture of MeOH (10 mL) and water (10 mL) was added methyl 5-cyano-2-methoxy-4-methylbenzoate (**42**, 700 mg, 3.41 mmol) followed by NaOH (1.36 g, 34.1 mmol). The mixture was stirred at room temperature for 30 h. The solution was then adjusted to pH=2 by addition of a 1N HCl solution, and the mixture was extracted with EtOAc (60 mL). Then the organic layer was washed with brine (20 mL), dried over Na<sub>2</sub>SO<sub>4</sub>, and concentrated under reduced pressure to afford the title compound (619 mg, 95%) as a white solid. <sup>1</sup>H NMR (400 MHz, CDCl<sub>3</sub>): δ 8.37 (s, 1H), 6.98 (s, 1H), 4.11 (s, 3H), 2.62 (s, 3H). MS m/z 192 [M+H]<sup>+</sup>.

*5-cyano-N-(6-(4-isopropyl-4H-1,2,4-triazol-3-yl)pyridin-2-yl)-2-methoxy-4-methylbenzamide (44)*. To a solution of 5-cyano-2-methoxy-4-methylbenzoic acid (**43**, 200 mg, 1.05 mmol) in acetonitrile (4mL) was added DMF (45.9 mg, 0.63 mmol) and oxalyl chloride (139 mg, 1.10 mmol). The mixture was stirred at room temperature for 1 h, at which time it turned into an orange solution. Then 6-[4-(propan-2-yl)-4H-1,2,4-triazol-3-yl]pyridin-2-amine (**5**, 212 mg, 1.04 mmol) was added in portions. The reaction mixture was stirred at room temperature for 30 minutes and the resulting heterogeneous mixture was filtered. The filter cake was washed with petroleum ether (3\*3 mL), and dried under reduced pressure to afford the title compound (333 mg, 85%) as a white solid. <sup>1</sup>H NMR (400 MHz, DMSO-d<sub>6</sub>): δ 10.71 (s, 1H), 9.84 (s, 1H), 8.34 (d, J=8.0 Hz, 1H), 8.20 - 8.08 (m, 2H), 8.00 - 7.96 (m, 1H), 7.38 (s, 1H), 5.31 - 5.18 (m, 1H), 3.99 (s, 3H), 2.55 (s, 3H), 1.54 (d, J=6.5 Hz, 6H). MS m/z 377 [M+H]<sup>+</sup>.

*N1-(6-(4-isopropyl-4H-1,2,4-triazol-3-yl)pyridin-2-yl)-6-methoxy-4-methylisophthalamide (45)*. To a solution of 5-cyano-2-methoxy-4-methyl-N-{6-[4-(propan-2-yl)-4H-1,2,4-triazol-3-yl]pyridin-2-yl}benzamide (**44**, 160 mg, 0.42 mmol) in DMSO (20 mL) were added K<sub>2</sub>CO<sub>3</sub> (294 mg, 2.13 mmol) and H<sub>2</sub>O<sub>2</sub> (30% w/w solution in water, 2.13 mmol) at room temperature. The pale yellow reaction mixture was stirred at this temperature for 30 minutes. Then

the reaction mixture was diluted with water (10 mL). The mixture was extracted with EtOAc (3\*20 mL). The combined organic layers were dried over Na<sub>2</sub>SO<sub>4</sub>, filtered, concentrated to dryness to give the crude which was purified by preparative HPLC (DuraShell 150\*25mm\*5µm; gradient from 19% to 39% MeCN in water (0.225% FA) in 11 minutes; flow rate: 30 mL/min) to afford the title compound (7.7 mg, 5%) as a white solid. <sup>1</sup>H NMR (400 MHz, DMSO-d<sub>6</sub>): δ 10.56 (s, 1H), 8.90 (s, 1H), 8.32 (d, J=8.0 Hz, 1H), 8.07 - 7.99 (m, 2H), 7.87 (d, J=7.5 Hz, 1H), 7.80 (br. s., 1H), 7.34 (br. s., 1H), 7.16 (s, 1H), 5.49 (td, J=6.7, 13.2 Hz, 1H), 4.02 (s, 3H), 2.49 (s, 3H), 1.52 (d, J=6.5 Hz, 6H). <sup>13</sup>C NMR (500 Mhz, DMSO-d<sub>6</sub>): 170.36, 163.67, 157.84, 151.35, 150.26, 146.69, 143.79, 143.35, 140.40, 130.86, 129.99, 119.62, 119.06, 114.14, 114.40, 57.08, 49.71, 23.66, 20.76. MS m/z 395 [M+H]<sup>+</sup>. HRMS for C<sub>20</sub>H<sub>23</sub>N<sub>6</sub>O<sub>3</sub> [M+H]<sup>+</sup>: calc. 395.1826, exp. 395.1824.

*5-mercapto-2-methoxy-4-methylbenzoic acid (13)*. A solution of 5-(chlorosulfonyl)-2-methoxy-4-methylbenzoic acid (**11**, 1.0 g, 3.8 mmol) in AcOH (3 mL) was stirred and heated at 90 °C for 10 minutes. Then the reaction was cooled to 45 °C. Sn (1.57 g, 13.2 mmol) and HCl (7 mL) were then successively added. The reaction mixture was heated to 60 °C for 2 hours. The mixture was allowed to cool to room temperature and was poured into water (20 mL). The precipitate was filtered off, washed with water and dried under vacuo to afford the title compound (740 mg, 99%) as an off-green solid and was used as is in the next step without further purification. <sup>1</sup>H NMR (400 MHz, DMSO-d<sub>6</sub>): δ 12.52 (br. s, 1H), 7.68 (s, 1H), 7.01 (s, 1H), 3.77 (s, 3H), 2.29 (s, 3H). MS m/z 199 [M+H]<sup>+</sup>.

*methyl 2-methoxy-4-methyl-5-(methylthio)benzoate (14)*. A white mixture of 2-methoxy-4-methyl-5-sulfanylbenzoic acid (**13**, 100 mg, 0.504 mmol), MeI (215 mg, 1.51 mmol) and K<sub>2</sub>CO<sub>3</sub> (209 mg, 1.51 mmol) in acetone (5 mL) was stirred at 50 °C for 16 hours. The white mixture was filtered and the filtrate was concentrated under reduced pressure. The residue was purified by flash chromatography over silica gel (MeOH/DCM from 0/100 to 1/99) to afford the title compound (30 mg, 26%) as a white solid. <sup>1</sup>H NMR (400 MHz, CDCl<sub>3</sub>): δ 7.72 (s, 1H), 6.82 (s, 1H), 3.89 (s, 6H), 2.43 (s, 3H), 2.41 (s, 3H). MS m/z 227 [M+H]<sup>+</sup>.

*methyl 2-methoxy-4-methyl-5-(methylsulfonyl)benzoate (15)*. A solution of methyl 2-methoxy-4-methyl-5-(methylsulfanyl)benzoate (**14**, 100 mg, 0.442 mmol), benzoic acid (54.0 mg, 0.442 mmol) and benzyltriethylammonium chloride (10.1 mg, 0.0442 mmol) in DCM (1 mL) at 20 °C was stirred vigorously with KMnO<sub>4</sub> (210 mg, 1.33 mmol) in water (2 mL) for 3 hours. Solid Na<sub>2</sub>S<sub>2</sub>O<sub>5</sub> was added until colorless mixture, which was then filtered through Celite. The organic layer was separated and the aqueous layer was washed with DCM

(3\*20 mL). The combined organic extracts were washed with an aqueous 1M H<sub>2</sub>NNH<sub>2</sub>·2HCl solution (30 mL), followed by saturated Na<sub>2</sub>CO<sub>3</sub> (30 mL) and brine (30 mL), dried over Na<sub>2</sub>SO<sub>4</sub> and filtered. The filtrate was evaporated under reduced pressure to afford the title compound (86 mg, 75%) as a white solid. <sup>1</sup>H NMR (400 MHz, CDCl<sub>3</sub>): δ 8.49 (s, 1H), 6.90 (s, 1H), 3.99 (s, 3H), 3.90 (s, 3H), 3.08 (s, 3H), 2.74 (s, 3H). MS m/z 259 [M+H]<sup>+</sup>.

*2-methoxy-4-methyl-5-(methylsulfonyl)benzoic acid (16)*. A mixture of methyl 2-methoxy-4-methyl-5-(methylsulfonyl)benzoate (**15**, 86 mg, 0.33 mmol) and LiOH·H<sub>2</sub>O (69.9 mg, 1.66 mmol) in THF (4 mL), EtOH (1 mL) and water (1 mL) was stirred at 20 °C for 5 hours. The mixture was filtered and the filtrate was evaporated. The residue was dissolved in water (10 mL) and acidified with a 1N HCl solution until pH=4, at which time a precipitate formed. The mixture was filtered and the solid was washed with water and dried under vacuo to afford the title compound (81 mg, 100%) as a white solid. <sup>1</sup>H NMR (400 MHz, CD<sub>3</sub>OD): δ 8.42 (s, 1H), 7.17 (s, 1H), 3.98 (s, 3H), 3.13 (s, 3H), 2.74 (s, 3H). MS m/z 245 [M+H]<sup>+</sup>.

*2-methoxy-4-methyl-5-(methylsulfonyl)-N-[6-[4-(propan-2-yl)-4H-1,2,4-triazol-3-yl]pyridin-2-yl]benzamide (21)*. To a solution of 2-methoxy-4-methyl-5-(methylsulfonyl)benzoic acid (**16**, 81 mg, 0.33 mmol) and oxalyl chloride (84.2 mg, 0.663 mmol) in acetonitrile (8 mL) was added DMF (0.1 mL). The reaction mixture was stirred at 20 °C for 2 hours and 50 °C for 2 hours. The now yellow solution was then cooled down to room temperature. Volatiles were evaporated under reduced pressure to give the acid chloride intermediate (87 mg, 100%) as a gum which was used in next step immediately. A yellow solution of this gum, 6-[4-(propan-2-yl)-4H-1,2,4-triazol-3-yl]pyridin-2-amine (**5**, 67.3 mg, 0.331 mmol) and pyridine (26.2 mg, 0.331 mmol) in acetonitrile (10 mL) was stirred at 20 °C for 16 hours. The reaction became a yellow suspension. The mixture was quenched with water (0.1 mL) and concentrated under reduced pressure. The residue was purified by preparative HPLC (Luna C18 150\*25\*5μm; gradient from 28% to 48% MeCN in water (0.225% FA); 35 mL/min) to afford the title compound (11 mg, 8%) as an off-white solid. <sup>1</sup>H NMR (400 MHz, DMSO-d<sub>6</sub>): δ 10.57 (s, 1H), 8.90 (s, 1H), 8.37 (s, 1H), 8.29 (d, J=8.0 Hz, 1H), 8.05 (t, J=8.0 Hz, 1H), 7.89 (d, J=8.0 Hz, 1H), 7.38 (s, 1H), 5.51 (sept, J=6.8 Hz, 1H), 4.06 (s, 3H), 3.23 (s, 3H), 2.72 (s, 3H), 1.51 (d, J=6.5 Hz, 6H). <sup>13</sup>C NMR (500 Mhz, DMSO-d<sub>6</sub>): 160.55, 151.17, 150.22, 146.63, 144.2, 143.8, 140.44, 132.4, 131.91, 120.86, 119.82, 116.95, 114.63, 57.57, 48.73, 44.04, 23.65, 20.51. MS m/z 430 [M+H]<sup>+</sup>.

## Biological Assays

### Evaluation of Inhibitory Activity against Full-length Recombinant Human ASK1

ASK1 enzyme activity was measured using the KinEASE™ Homogeneous Time Resolved Fluorescence assay (HTRF®, CisBio US), with full-length recombinant human ASK1 (MAP3K5, ThermoFisher Scientific). Dilution series of test compounds were prepared in 100% DMSO and 200 nL were dispensed to the individual wells of a multiwell plate. ASK1 enzyme was diluted to 6 nM in 1X kinase buffer (Cisbio US) supplemented with 5 mM MgCl<sub>2</sub> and 1 mM DTT and 5 μL were added to the assay plate containing test compound. Test compounds were allowed to pre-incubate with ASK1 enzyme for 15 minutes at room temperature (25 °C). Next, 5 μL of 2 mM ATP and 2 μM STK3 peptide substrate (Cisbio US) in 1X supplemented kinase buffer were added to the assay plate to start the phosphorylation reaction. Assay plates were incubated for 90 min at room temperature and stopped by the addition of 10 μL of detection buffer containing EDTA, 1:200 STK-antibody-cryptate and 62.5 nM streptavidin-XL665 (Cisbio US). The assay plates were incubated for an additional 2 h at room temperature and then read on an EnVision Model 2104 plate reader using a 340 nm excitation wavelength and 665 nm (XL665) emission wavelength / 620 nm (cryptate) emission for fluorescence detection. The final amount of enzyme in the assay was 3 nM ASK1, the final concentration of STK3 peptide substrate (Serine/Threonine kinase 3, Cisbio US) was 1 μM and the final concentration of DMSO was 2%. The K<sub>m</sub> for ATP was determined to be 48 μM and utilized in calculations where appropriate. IC<sub>50</sub> curves were fit using a 4-parameter sigmoidal model. The K<sub>i</sub><sup>app</sup> was calculated by fitting the enzyme inhibition versus inhibitor concentration data to the Morrison equation (equation 9.6 in Copeland<sup>30</sup>) for tight binding inhibitors (**18-21, 31, 36, 38 and 45**) or the competitive inhibition equation (equation 8.1 in Copeland<sup>30</sup>) for weaker inhibitors (**25-27**). For SAR interpretation purposes, the K<sub>i</sub><sup>app</sup> values were converted to IC<sub>50</sub> values using the Cheng-Prusoff equation (equation 3 in Cheng and Prusoff<sup>32</sup>).

### Generation of ASK1 and ASK1 K709R Overexpressing Cells

Human full-length ASK1 was over-expressed in HEK293 cells containing a stress-activated luciferase reporter downstream of the transcription factor Activator Protein-1 (AP-1). AP-1 acts downstream of the stress-activated protein kinase/Jun N-terminal kinase (SAPK/JNK), hence the expectation was that activation of overexpressed ASK1 would lead to a robust reporter cell line for ASK1 kinase activity via MMK4 or MKK7 in this cell line, henceforth called HEK293/AP-1<sub>luc</sub>. Despite the constitutive activation of ASK1 in the overexpressing cells, AP-1-

induced luciferase expression was not detected in cells. This was supported by the failure to detect phosphorylated JNK (data not shown). Instead, in this cell system, constitutively activated ASK1 resulted in elevated phosphorylation of p38, the other ASK1-dependent substrate via MKK3 and MKK6.<sup>7</sup>

HEK293/AP-1<sub>luc</sub> cells were cultured in Eagle's Minimum Essential Medium (ATCC), containing 10% fetal bovine serum, 100 U/mL penicillin-100 µg/mL streptomycin solution, 500 µg/mL Geneticin (ThermoFisher Scientific), and 1 µg/mL puromycin (Sigma Aldrich). Cells were incubated at 37 °C, 5% CO<sub>2</sub>, 95% humidity and medium changed weekly or as needed. To express ASK1, HEK293/AP-1<sub>luc</sub> cells were transfected with human, full-length ASK1 in pcDNA3.1 (wild type or catalytically inactive K709R) using the Lipofectamine 2000 transfection kit according to manufacturer's instructions. Following transfection, clones were grown in the presence of 500 µg/mL Geneticin and a stable pool was generated from the cells resistant to the antibiotic. The expression of ASK1 was further characterized by western blot.

#### **Characterization of ASK1 and ASK1 K709R Overexpressing Cells by Western Blot**

Parental HEK293/AP-1<sub>luc</sub> cells or cells overexpressing wild type or K709R mutant human full-length ASK1 were plated in DMEM containing 10% Fetal bovine serum, 100 U/mL penicillin, 100 µg/mL streptomycin, 500 µg/mL Geneticin, and 1 µg/mL puromycin (Sigma Aldrich). The following day, in preparation for inhibitor treatment, the cells were washed once with medium containing no FBS. Inhibitor **38** was diluted in culture medium to give a final concentration of 10 µM and 3 mL of the medium were transferred to the cells. Cells were allowed to incubate at 37 °C for 30 minutes before being harvested. Cells were washed with PBS and pelleted. Mammalian Protein Extraction lysis buffer (M-PER, ThermoFisher Scientific) containing the Halt protease and phosphatase inhibitors was used to lyse the cells and protein estimation was performed using the BCA method before analyzing the cell lysates by Western blot. Antibodies to human ASK1, phospho-Thr838 in human ASK1 and α-Tubulin (Cell Signaling Technologies) were used to detect the protein bands.

#### **Evaluation of Intracellular Inhibitory Activity against ASK1 overexpressed in HEK293/AP-1<sub>luc</sub> cells**

Intracellular ASK1 enzyme activity was measured using the phospho-p38 Homogeneous Time Resolved Fluorescence assay kit (HTRF®, CisBio US). For the assay, cells over-expressing wild-type ASK1 were cultured to near confluence in supplemented Eagle medium, harvested and seeded into white, Poly D-Lysine-coated, 384-well, sterile plates (Greiner) at 25K cells/well. Cell plates were incubated at 37 °C, 5% CO<sub>2</sub>, 95% humidity for a period of 8 h. Then, the cell plates were removed from incubation and the medium was exchanged for Optimem supplemented with Geneticin (ThermoFisher Scientific).

Dilution series of test inhibitors were solubilized in 100% DMSO. Compounds were prepared as a 200-fold multiple of the final in-assay concentration with a final DMSO concentration of 0.5%. Next, 2 µL of serialized test inhibitor dilution series were added into ultra-clear polypropylene, 384-well, U-bottom assay plates (Corning Life Sciences). A step-down dilution into supplemented Optimem was performed and 5 µL of diluted inhibitor or control compound is added to the corresponding wells of the cell plates. The treated cell plates were incubated at 37 °C, 5% CO<sub>2</sub>, 95% humidity for a period of 18 h. Following the 18 h incubation, cell plates were briefly spun at 1000 rpm using an Eppendorf 5804R swinging-bucket centrifuge for 1 min and the medium was exchanged for 1X Lysis buffer. The cell plates containing lysis buffer were incubated for 1 h at room temperature while shaking at 700 rpm on an orbital shaker. Afterward, the cell plates were briefly spun again at 1000 rpm for 1 min and 16 µL of the lysate from each well were transferred to the a white, 384-well, small-volume detection plate (Greiner) containing 2 µL of each of the anti-phospho-p38 antibodies according to manufacturer's instructions (Cisbio US). The detection plates were incubated overnight (18 h) at room temperature and then read on an EnVision Model 2104 plate reader using a 340 nm excitation wavelength and 665 nm (XL665) emission wavelength / 620 nm (cryptate) emission for fluorescence detection.

#### Associated Content

## Supporting Information

Material supplied as Supporting Information includes animal pharmacokinetics, kinase selectivity data, protein crystallography methods and refinement statistics, docking procedure and torsion plots (PDF).

Molecular formula strings (CSV).

### Accession Codes

Protein crystal coordinates for ASK1 complexes with **18** (5VIL) and **19** (5VIO) have been deposited in the RCSB. Authors will release the atomic coordinates and experimental data upon article publication. See Supplementary Information for methods and refinement statistics.

## Acknowledgements

The authors would like to acknowledge Jamie Smith for supplying ASK1 plasmids and Sheila Kantesaria for supplying the AP1 luciferase cell line.

## Abbreviations used

AP-1 – Activator Protein-1

ASK1 – Apoptosis signal-regulating kinase 1

JNK – Jun N-terminal kinase

ROS – Reactive oxygen species

SFlogD – shake flask logD

TRX – thioredoxin

## References

1. Zhang, W.; Liu, H. T., MAPK signal pathways in the regulation of cell proliferation in mammalian cells. *Cell. Res.* **2002**, *12*, 9-18.
2. Tobiume, K.; Matsuzawa, A.; Takahashi, T.; Nishitoh, H.; Morita, K.; Takeda, K.; Minowa, O.; Miyazono, K.; Noda, T.; Ichijo, H., ASK1 is required for sustained activations of JNK/p38 MAP kinases and apoptosis. *EMBO Rep.* **2001**, *2*, 222-228.
3. Nishitoh, H.; Saitoh, M.; Mochida, Y.; Takeda, K.; Nakano, H.; Rothe, M.; Miyazono, K.; Ichijo, H., ASK1 is essential for JNK/SAPK activation by TRAF2. *Mol. Cell.* **1998**, *2*, 389-395.
4. Ichijo, H.; Nishida, E.; Irie, K.; ten Dijke, P.; Saitoh, M.; Moriguchi, T.; Takagi, M.; Matsumoto, K.; Miyazono, K.; Gotoh, Y., Induction of apoptosis by ASK1, a mammalian MAPKKK that activates SAPK/JNK and p38 signaling pathways. *Science* **1997**, *275*, 90-94.
5. Matsuzawa, A.; Saegusa, K.; Noguchi, T.; Sadamitsu, C.; Nishitoh, H.; Nagai, S.; Koyasu, S.; Matsumoto, K.; Takeda, K.; Ichijo, H., ROS-dependent activation of the TRAF6-ASK1-p38 pathway is selectively required for TLR4-mediated innate immunity. *Nat. Immunol.* **2005**, *6*, 587-592.
6. Matsuzawa, A.; Ichijo, H., Molecular mechanisms of the decision between life and death: regulation of apoptosis by apoptosis signal-regulating kinase 1. *J. Biochem.* **2001**, *130*, 1-8.
7. Hayakawa, R.; Hayakawa, T.; Takeda, K.; Ichijo, H., Therapeutic targets in the ASK1-dependent stress signaling pathways. *Proc. Jpn. Acad. Ser. B Phys. Biol. Sci.* **2012**, *88*, 434-453.
8. Nishitoh, H.; Matsuzawa, A.; Tobiume, K.; Saegusa, K.; Takeda, K.; Inoue, K.; Hori, S.; Kakizuka, A.; Ichijo, H., ASK1 is essential for endoplasmic reticulum stress-induced neuronal cell death triggered by expanded polyglutamine repeats. *Genes Dev.* **2002**, *16*, 1345-1355.
9. Saitoh, M.; Nishitoh, H.; Fujii, M.; Takeda, K.; Tobiume, K.; Sawada, Y.; Kawabata, M.; Miyazono, K.; Ichijo, H., Mammalian thioredoxin is a direct inhibitor of apoptosis signal-regulating kinase (ASK) 1. *EMBO J.* **1998**, *17*, 2596-2606.

10. Gotoh, Y.; Cooper, J. A., Reactive oxygen species- and dimerization-induced activation of apoptosis signal-regulating kinase 1 in tumor necrosis factor-alpha signal transduction. *J. Biol. Chem.* **1998**, *273*, 17477-17482.
11. Bunkoczi, G.; Salah, E.; Filippakopoulos, P.; Fedorov, O.; Muller, S.; Sobott, F.; Parker, S. A.; Zhang, H.; Min, W.; Turk, B. E.; Knapp, S., Structural and functional characterization of the human protein kinase ASK1. *Structure* **2007**, *15*, 1215-1226.
12. Takada, E.; Furuhashi, M.; Nakae, S.; Ichijo, H.; Sudo, K.; Mizuguchi, J., Requirement of apoptosis-inducing kinase 1 for the induction of bronchial asthma following stimulation with ovalbumin. *Int. Arch. Allergy Immunol.* **2013**, *162*, 104-114.
13. Terada, Y.; Inoshita, S.; Kuwana, H.; Kobayashi, T.; Okado, T.; Ichijo, H.; Sasaki, S., Important role of apoptosis signal-regulating kinase 1 in ischemic acute kidney injury. *Biochem. Biophys. Res. Commun.* **2007**, *364*, 1043-1049.
14. Izumiya, Y.; Kim, S.; Izumi, Y.; Yoshida, K.; Yoshiyama, M.; Matsuzawa, A.; Ichijo, H.; Iwao, H., Apoptosis signal-regulating kinase 1 plays a pivotal role in angiotensin II-induced cardiac hypertrophy and remodeling. *Circ. Res.* **2003**, *93*, 874-883.
15. Yamaguchi, O.; Higuchi, Y.; Hirotsu, S.; Kashiwase, K.; Nakayama, H.; Hikoso, S.; Takeda, T.; Watanabe, T.; Asahi, M.; Taniike, M.; Matsumura, Y.; Tsujimoto, I.; Hongo, K.; Kusakari, Y.; Kurihara, S.; Nishida, K.; Ichijo, H.; Hori, M.; Otsu, K., Targeted deletion of apoptosis signal-regulating kinase 1 attenuates left ventricular remodeling. *Proc. Natl. Acad. Sci.* **2003**, *100*, 15883-15888.
16. Mnich, S. J.; Blanner, P. M.; Hu, L. G.; Shaffer, A. F.; Happa, F. A.; O'Neil, S.; Ukairo, O.; Weiss, D.; Welsh, E.; Storer, C.; Mbalaviele, G.; Ichijo, H.; Monahan, J. B.; Hardy, M. M.; Eda, H., Critical role for apoptosis signal-regulating kinase 1 in the development of inflammatory K/BxN serum-induced arthritis. *Int. Immunopharmacol.* **2010**, *10*, 1170-1176.

17. Yokoi, T.; Fukuo, K.; Yasuda, O.; Hotta, M.; Miyazaki, J.; Takemura, Y.; Kawamoto, H.; Ichijo, H.; Ogiwara, T., Apoptosis signal-regulating kinase 1 mediates cellular senescence induced by high glucose in endothelial cells. *Diabetes* **2006**, *55*, 1660-1665.
18. Toldo, S.; Breckenridge, D. G.; Mezzaroma, E.; Van Tassell, B. W.; Shryock, J.; Kannan, H.; Phan, D.; Budas, G.; Farkas, D.; Lesnefsky, E.; Voelkel, N.; Abbate, A., Inhibition of apoptosis signal-regulating kinase 1 reduces myocardial ischemia-reperfusion injury in the mouse. *J. Am. Heart Assoc.* **2012**, *1*, e002360.
19. Huang, Q.; Zhou, H. J.; Zhang, H.; Huang, Y.; Hinojosa-Kirschenbaum, F.; Fan, P.; Yao, L.; Belardinelli, L.; Tellides, G.; Giordano, F. J.; Budas, G. R.; Min, W., Thioredoxin-2 inhibits mitochondrial reactive oxygen species generation and apoptosis stress kinase-1 activity to maintain cardiac function. *Circulation* **2015**, *131*, 1082-1097.
20. Tesch, G. H.; Ma, F. Y.; Han, Y.; Liles, J. T.; Breckenridge, D. G.; Nikolic-Paterson, D. J., ASK1 Inhibitor halts progression of diabetic nephropathy in Nos3-deficient mice. *Diabetes* **2015**, *64*, 3903-3913.
21. Xie, Y.; Ramachandran, A.; Breckenridge, D. G.; Liles, J. T.; Lebofsky, M.; Farhood, A.; Jaeschke, H., Inhibitor of apoptosis signal-regulating kinase 1 protects against acetaminophen-induced liver injury. *Toxicol. Appl. Pharmacol.* **2015**, *286*, 1-9.
22. Terao, Y.; Suzuki, H.; Yoshikawa, M.; Yashiro, H.; Takekawa, S.; Fujitani, Y.; Okada, K.; Inoue, Y.; Yamamoto, Y.; Nakagawa, H.; Yao, S.; Kawamoto, T.; Uchikawa, O., Design and biological evaluation of imidazo[1,2-a]pyridines as novel and potent ASK1 inhibitors. *Bioorg. Med. Chem. Lett.* **2012**, *22*, 7326-7329.
23. Swinnen, D.; Jorand-Lebrun, C.; Grippi, V.; Vallotton, T.; Muzerelle, M.; Royle, A.; Macritchie, J.; Hill, R.; Shaw, J. P. Preparation of triazolopyridines as apoptosis signal-regulating kinase (ASK) inhibitors

for treatment of autoimmune, inflammatory, cardiovascular, and/or neurodegenerative diseases.

WO2009027283A1, 2009.

24. Chang, E. Preparation of pyrrolo[3,2-c]pyridine compounds as therapeutic apoptosis signal-regulating kinase 1 inhibitors. WO2011097079A1, 2011.

25. Notte, G. Preparation of N-[triazolylpyridinyl] benzamide derivs. as apoptosis signalregulating kinase inhibitors useful in the treatment of kidney disease. WO2013112741A1, 2013.

26. Bansal, R.; Nagorniewicz, B.; Prakash, J., Clinical advancements in the targeted therapies against liver fibrosis. *Mediators. Inflamm.* **2016**, *2016*, 1-16.

27. Ghose, A. K.; Herbertz, T.; Pippin, D. A.; Salvino, J. M.; Mallamo, J. P., Knowledge based prediction of ligand binding modes and rational inhibitor design for kinase drug discovery. *J. Med. Chem.* **2008**, *51*, 5149-5171.

28. Xing, L.; Klug-Mcleod, J.; Rai, B.; Lunney, E. A., Kinase hinge binding scaffolds and their hydrogen bond patterns. *Bioorg. Med. Chem.* **2015**, *23*, 6520-6527.

29. Edward, B.; Kazuhiko, S.; Teruaki, M., A facile synthesis of carboxamides by using 1-methyl-2-halopyridinium iodides as coupling reagents. *Chem. Lett.* **1975**, *4*, 1163-1166.

30. Copeland, R. A., *Enzymes: a practical introduction to structure, mechanism and data analysis* Second ed.; Wiley-VCH: New York, 2000.

31. Morrison, J. F., Kinetics of the reversible inhibition of enzyme-catalysed reactions by tight-binding inhibitors. *Biochim. Biophys. Acta* **1969**, *185*, 269-286.

32. Cheng, Y.; Prusoff, W. H., Relationship between the inhibition constant ( $K_1$ ) and the concentration of inhibitor which causes 50 per cent inhibition ( $I_{50}$ ) of an enzymatic reaction. *Biochem. Pharmacol.* **1973**, *22*, 3099-3108.

33. See supplemental material for detailed information.

34. Leeson, P. D.; Springthorpe, B., The influence of drug-like concepts on decision-making in medicinal chemistry. *Nat. Rev. Drug Discov.* **2007**, *6*, 881-890.
35. Ryckmans, T.; Edwards, M. P.; Horne, V. A.; Correia, A. M.; Owen, D. R.; Thompson, L. R.; Tran, I.; Tutt, M. F.; Young, T., Rapid assessment of a novel series of selective CB2 agonists using parallel synthesis protocols: a lipophilic efficiency (LipE) analysis. *Bioorg. Med. Chem. Lett.* **2009**, *19*, 4406-4409.
36. Di, L.; Whitney-Pickett, C.; Umland, J. P.; Zhang, H.; Zhang, X.; Gebhard, D. F.; Lai, Y.; Federico, J. J., 3rd; Davidson, R. E.; Smith, R.; Reyner, E. L.; Lee, C.; Feng, B.; Rotter, C.; Varma, M. V.; Kempshall, S.; Fenner, K.; El-Kattan, A. F.; Liston, T. E.; Troutman, M. D., Development of a new permeability assay using low-efflux MDCKII cells. *J. Pharm. Sci.* **2011**, *100*, 4974-4985.
37. Walters, W. P.; Green, J.; Weiss, J. R.; Murcko, M. A., What do medicinal chemists actually make? a 50-year retrospective. *J. Med. Chem.* **2011**, *54*, 6405-6416.
38. Li, R.; Bi, Y.-A.; Lai, Y.; Sugano, K.; Steyn, S. J.; Trapa, P. E.; Di, L., Permeability comparison between hepatocyte and low efflux MDCKII cell monolayer. *AAPS J.* **2014**, *16*, 802-809.
39. Sessel, S.; Fernandez, A., Selectivity filters to edit out deleterious side effects in kinase inhibitors. *Curr. Top. Med. Chem.* **2011**, *11*, 788-799.
40. See supplemental material for tabulated assay values.
41. Di, L.; Keefer, C.; Scott, D. O.; Strelevitz, T. J.; Chang, G.; Bi, Y.-A.; Lai, Y.; Duckworth, J.; Fenner, K.; Troutman, M. D.; Obach, R. S., Mechanistic insights from comparing intrinsic clearance values between human liver microsomes and hepatocytes to guide drug design. *Eur. J. Med. Chem.* **2012**, *57*, 441-448.
42. Bhattachar, S. N.; Wesley, J. A.; Seadeek, C., Evaluation of the chemiluminescent nitrogen detector for solubility determinations to support drug discovery. *J. Pharm. Biomed. Anal.* **2006**, *41*, 152-157.

A structural analysis of ASK1 found that there is a rare GLN756 at the GK+2 position.

Docking a library of 14K amides targeting GLN756 resulted in a promising lead.

Optimization resulted in compounds with cell potency and kinome selectivity.

ACCEPTED MANUSCRIPT